To design novel derivatives of noscapine (we called as fourth generation) using structure based computer aided molecular designing techniques

.

122504

Anuja Mishra

-Dr. Chittaranjan Rout

May 2012-2014

Submitted in partial fulfillment of the Degree of

Master of Technology

DEPARTMENT OF BIOTECHNOLOFY AND BIOINFORMATICS

JAYPEE UNIVERSITY OF INFORMATION TECHNOLOGY,

WAKNAGHAT

TALBLE OF CONTENTS

CERTIFICATE

This is to certify that the work titled "TO DESIGN NOVEL DERIVATEVS OF NOSCAPINE (we called as fourth generation) USING STRUCTURE BASED COMPUTER AIDED MOLECULER DESIGNING TECHNIQUE" submitted by "ANUJA MISHRA" in partial fulfillment for the award of degree of M. Tech of Jaypee University of Information Technology, Waknaghat has been carried out under my supervision. This work has not been submitted partially or wholly to any other University or Institute for the award of this or any other degree.

Signature of Supervisor

Name of Supervisor Dr. Chittaranjan Rout

Date 24/may/2014

ACKNOWLEDGEMENT

It is my pleasure to be indebted to various people, who directly or indirectly contributed in the development of this work and who influenced my thinking, behavior, and acts during the course of study.

I express my sincere gratitude to **Dr. Rajinder S. Chauhan** JAYPEE UNIVERSITY OF INFORMATION TECHNOLOGY for providing me an opportunity to work.

I am thankful to **Dr. Chittaranjan Rout** for his guidance, support, cooperation, and motivation provided to me, and for continuous inspiration, presence and blessings.

Lastly, I would like to thank the almighty and my parents for their moral support and my friends with whom I shared my day-to-day experience and received lots of suggestions that improved my quality of work.

Signature of the student ……..

Name of Student ANUJA MISHRA

Date …../May/2014

Abstract of dissertation

Microtubules are major cytoskeletal structures responsible for maintaining genetic stability during cell division. The dynamics of these polymers is absolutely crucial for this function. Interference with microtubules dynamics often leads to programmed cell death and thus microtubule-binding drugs such as paclitaxel, docetaxel and the vinca alkaloids are currently used to treat various malignancies in the clinic. However, these chemotherapy drugs are confounded by complications with toxicity, owing to their non-selective action and extreme overpolymerizing effects (taxanes) or depolymerizing effects (vincas) on microtubules. Besides toxicity, hydrophobic nature of these drugs confers insolubility necessitating the use of vehicles (such as Tween-80) that many a time cause extreme hypersensitivity reactions. Therefore, there is an urgent need to explore novel tubulin-binding agents that are significantly effective and comparatively less toxic compared to currently available drugs. Systematic screening of new compounds that interfere with microtubules, noscapine, an opium alkaloid was discovered that binds stoichiometrically to tubulin, alters its conformation upon binding and arrests mammalian cells in mitosis. It was also shown that unlike many other microtubule inhibitors, noscapinoids does not significantly promote or inhibit microtubule polymerization; instead, they alters the steady-state dynamics of microtubule assembly, primarily by increasing the amount of time that the microtubules spend in an attenuated (pause) state. As a result of this and compromised checkpoints cancer cells selectively get killed by noscapinoids, while unaffecting the normal cells. Furthermore, noscapine causes apoptosis in many cancer cell types and has potent anti-tumor activity against solid tumors in nude mice. In addition, noscapine has some other advantage properties as lead molecule: (1) retains activity against paclitaxel-resistant cell lines (1A9/PTX10, 1A9/PTX22) and epothilone-resistant cell line (1A9/A8); (2) a favourable pharmacokinetics (clearance in 6-10 hours); (3) a poor substrate for drug-pumps (polyglycoprotiens and MDR-related proteins) that comprise a major cause of drug resistance; (4) it do not show immunological and neurological toxicities and (5) inhibit tumorigenesis *in vivo* albeit at high concentrations (~ 300 mg/kg body weight). Although noscapine is cytotoxic in a variety of different cancer cell lines (NCI 60 cell lines panel),

the IC_{50} values remain in the high micromolar ranges (~21.1 to 100 μM). To enhance its activity further, efforts have been focused on rational drug design and synthesis of new generation of noscapine derivatives (we called as noscapinoids) for the better therapeutic outcome.

With this objective in this dissertation a new series of noscapine derivatives consisting of 18 compounds has been designed using combinatorial module of Schrodinger. All these derivatives showed improved docking score ranging from -5.8 kcal/mol to -8.17 kcal/mol compared to the lead molecule, noscapine. The predictive binding affinity calculated based on MM-GBSA also revealed improved ΔGbind ranging from -45.12 kcal/mol to -100.75 kcal/mol. Collectively, the study reported here identified potential derivatives of noscapine pertaining to chemical synthesis and experimental evaluation as anti-cancer drugs.

Chapter-1

Introduction

Cancer is one of the leading cause of death in the India (Table **1**). It is a class of diseases in which a group of cells display uncontrolled growth, invasive intrusion, destruction of adjacent tissues, and metastasis to other locations in the body via lymph and/or blood. Cancer may affect people at all ages, even fetuses, but the risk for most varieties increases with age through out the world (Fig. **1**). While a cure for cancer is still a dream, considerable advances have been made in curbing the suffering and the progression of this devastating disease, which has taken the centre stage in the arena of healthcare

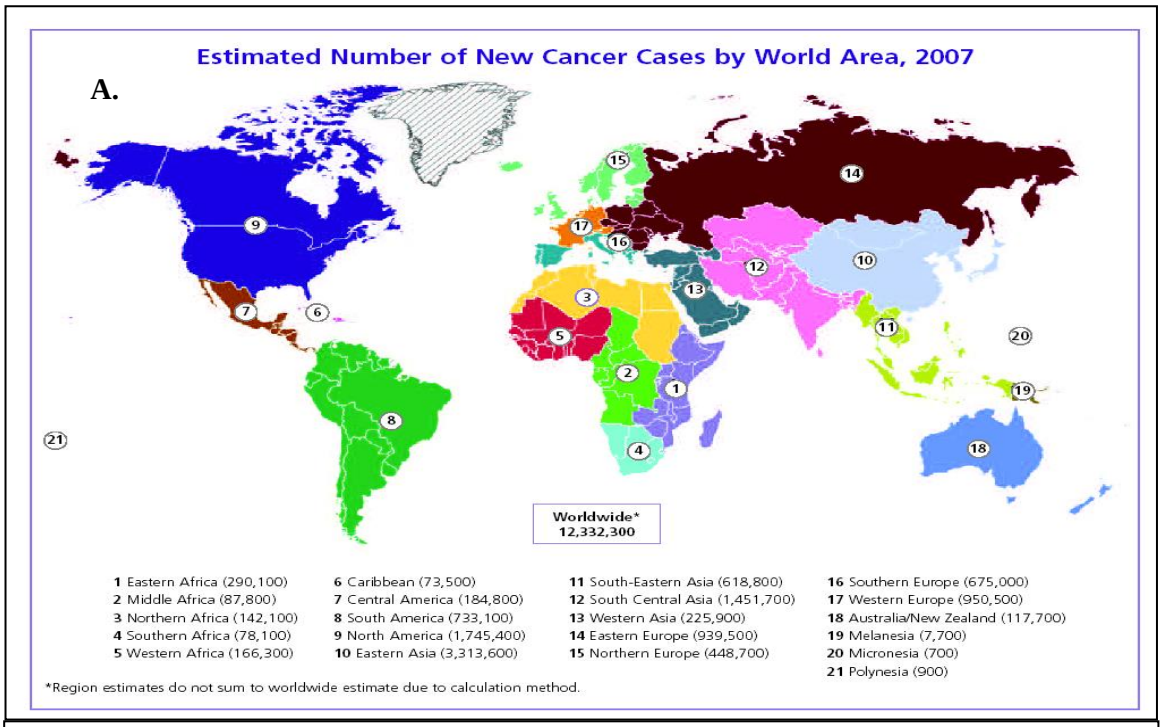

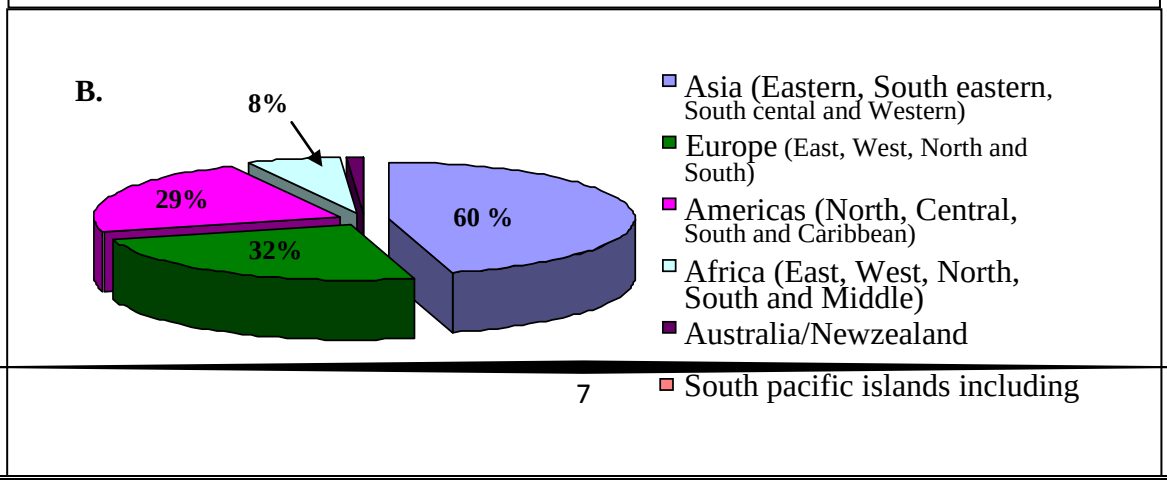

professionals.

Figure 1. Continental distribution of cancer cases.

(A). Visual depiction of the estimates projected by the American Cancer society in 2007.

(B). Compilation of data from panel A. This compilation clearly notes Asia as the leader with 5.6 million cases followed immediately by Europe and Americas with 3.0 and 2.7 millions respectively. Africa notes only around 764 thousand cases. (This surprisingly low figure might represent under diagnosis.) Interestingly, Australia-New Zealand taken together projected only around 117 thousand cases. This figure, presents the stark realization that cancer cannot be viewed as a disease of wealthy, and it should be a united global effort to find curative/palliative measures. Data presentation (A) adapted with permission from American Cancer Society: Global facts and figures 2007. Atlanta: American Cancer Society, Inc.

Chapter-2

DEVELOPMENTS IN THE FIELD OF CANCER TREATMENT

Cancer cells usually escape the normal control of cell division cycle and programmed cell death due to either a direct effect on the cell-cycle and apoptotic machineries, or the signaling pathways that control them. Enormous heterogeneity in the genetic make-up and the context in which they affect cancer development and progression makes it difficult to design effective treatments. Chemotherapy and radiation therapy are conventional methods to treat metastatic cancer that are not amenable to surgical removal, with a major drawback of managing with severe side effects. These therapies cannot differentiate much between the normal and the cancerous cells and hence harm the normal cells as well, during the treatment. Comparatively newer method of cancer treatment is targeted cancer therapy that uses drugs or other substances (monoclonal antibodies, cytokines, etc.) to identify and attack cancer cells while doing little damage to normal cells.

Surgery and Radiation: Even today, surgery is the most common means of removing accessible tumors and this method remains mainstay of treatment for these kinds of tumors. However, many types of cancers remain surgically unapproachable. Hence the radiation therapy becomes necessary to ablate such localized tumors. Both the surgical and radiation arena are now witnessing major technical advances such as robot- and video- assisted and laparoscopic surgical procedures that are minimally invasive [4, 5, 6]; similarly, advances in radiation types and the precision in their targeted delivery to the tumor site have improved the effectiveness by limiting radiation exposure of healthy tissues [7]. Nevertheless, in both of these cases, there are limitations of removing or destroying only the bulk of the tumor mass and leaving behind residual tumor cells in the vicinity of the main tumor mass. Thus, these treatments often are followed by chemotherapy.

Chemotherapy: Chemotherapy is the general term for any treatment involving the use of chemical agents to stop cancer cells from growing. These chemical agents can work by any of the mechanisms such as interfering with DNA metabolism, cell division or signal transduction. Because of the systemic administration and generalized bioavailability, these treatment regimens can eliminate cancer cells at sites great distances from the original cancer. Chemotherapy remains a widely used means of treatment, prevention of reoccurrence and palliative care for a variety of cancer types. Therefore, not surprisingly over half of the patients diagnosed with cancer, receive chemotherapy. Conventionally, these types of agents were identified from the libraries of naturally derived compounds or of chemically synthesized compounds by evaluating their cytotoxicities to identify the promising lead compounds. The technical advances in the robotics, very sensitive yet simple assay systems, and state of the art development in combinatorial chemistry have now become a mainstay of this line of research. In addition, further advances in chirally biased chemical synthetic techniques and the advances in the separation of chiral compounds have now opened up novel vistas in this area. Basically, the drugs that are simply identified by cytotoxicity towards cancer cells do not particularly target the cancer cells exclusively and can equally be cytotoxic to normally dividing cells of the healthy tissues. Although highly cytotoxic, some of these drugs still remain most effective against complex solid tumors such as ovarian and breast as well as some hematological cancers [8].

Molecular identity of agents responsible for inter-organ and inter-tissue communication such as hormones (e.g. EGF), their receptors at the exposed cellular surfaces of the target tissues (e.g. HER2 receptor) and components of the intracellular molecular network responsible for amplifying the tiny event on the cellular surfaces, have now offered to specifically target these crucial events in an organ/tissue specific manner. In addition, because of the enzymatic amplification power of many players of the signal transduction pathways, the absolute levels of each protein is exclusively controlled often by their ubiquitination and proteosome mediated degradation, and this knowledge has also contributed to targeted approaches. For example Gleevec® (STI–571 or imatinib mesylate, targeting brc-abl), Iressa® (ZD1839 or gefitinib, targeting Erb B) and Velcade® (bortezomib, targeting proteosome) are few of the FDA approved targeted drugs that have been extremely useful in selected malignancies.

Immunotherapy: The immune system, responsible for protection against a variety of disease can also be augmented or exploited for the prevention or slowing down the growth and spread of tumors. Although there is clear evidence for a definite role of immune system in dampening the rate at which the tumor burden increases or its spread from the site of origin, the precise nature and the specific mechanisms involved are still being actively pursued. Many clinical trials of new forms of immunotherapy are in progress, an enormous amount of research still remains to be done before the findings can be widely applied. Some of the important immunotherapies are:

A). Monoclonal Antibodies: Ever since the invention in 1970's of producing antibodies from single cell clones (hybridomas that are produced by fusing individual antibody producing mouse B-cells with a uncontrollably growing mouse myeloma cells), the possibility of the use for cancer therapy is becoming a reality year by year [9, 10]. A major advance in this field is the ability to convert these antibodies, which originally were made from mouse hybridomas, to "humanized" antibodies that more closely resemble our natural antibodies. Even newer techniques can be used to generate human antibodies from genetically engineered mice or bacteria containing human antibody genes [11]. Monoclonal antibodies have been widely used in scientific studies and diagnosis of cancer. Intravenously injected monoclonal antibodies can seek out cancer cells in the patient's

body, and lead to disruption of intracellular activities and/or enhancement of further immune responses. After many years of clinical testing, researchers have proven that improved monoclonal antibodies can be used effectively to help treat certain cancers. For example, Rituximab (Rituxan) is useful in the treatment of non-Hodgkin's lymphoma [12], while trastuzumab (Herceptin) is useful against certain breast cancers [13, 14]. Other new monoclonal antibodies are undergoing active clinical trials and testing. The approved therapeutics have not only paved a way for more of simple antibodies as therapeutics emerge, but they are now providing basis to carry payloads such as toxins, other drugs, prodrugs, radioisotopes and nanoparticles to the cellular targets.

B). Cytokine Therapy: Cytokines are the messengers of the immune system. These are either proteins or glycoproteins secreted by immune cells and function locally in an autocrine manner or at a distance in a paracrine manner, to enhance or suppress immunity. As anti-cancer therapy, cytokines are used to enhance immunity. IL-2 and IFN-α 2b are two cytokines approved by the FDA for treatment of cancer. While IL-2 has demonstrated activity against renal cell, melanoma, lymphoma, and leukemia [15], IFN-α 2b has shown activity in the same pathologies but also in Kaposi's sarcoma, chronic myelogenous leukemia, and hairy cell leukemia [16].

C). Cancer Vaccines: Vaccines have revolutionized public health by preventing the development of many important infectious diseases, including polio, small pox, and diphtheria. It has been much more difficult to develop effective vaccines to prevent cancer, or to treat patients who already have cancer [17]. Attempts to develop such cancer vaccines, despite many decades of experimental work, have yet to yield proven results. In spite of this, a notable increase in interest has been generated by recent advances in the areas of immunology and cancer biology, which have led to more sophisticated and promising vaccine strategies than those previously available. Cancer vaccines typically consist of a source of cancer-associated antigen, along with other components, to further stimulate the immune response against the antigen [18]. There are two broad types of cancer vaccines. Preventive (or prophylactic) vaccines, which are intended to prevent

cancer from developing in healthy people; and Therapeutic vaccines, which are intended to treat already existing cancers by strengthening the body's natural defenses against cancer [19]. The U.S. Food and Drug Administration (USFDA) has approved Hepatitis B virus (HBV) vaccine as a cancer preventive vaccine, which protects against HBV infection that can lead to liver cancer. The first HBV vaccine was approved in 1981, making it the first cancer preventive vaccine to be successfully developed and marketed. Today, most children in the United States are vaccinated against HBV shortly after birth [20, 21]. In 2006, the USFDA approved the vaccine known as Gardasil®, which protects against infection by two types of human papilloma virus (HPV): specifically types 16 and 18 that cause approximately 70 percent of all cases of cervical cancer worldwide. At least 17 other types of HPV are responsible for the remaining 30 percent of cervical cancer cases [22]. Gardasil® also protects against HPV types 6 and 11, which are responsible for about 90 percent of all cases of genital warts. However, these two HPV types do not cause cervical cancer. In 2008, the FDA expanded Gardasil's approval to include its use in the prevention of HPV-associated vulvar and vaginal cancers also [NCI facts sheet]. Although there is progress in field of preventive cancer vaccines; however, cancer treatment vaccines still remain an experimental form of therapy.

As discussed above, in recent years many new targets are being studied for their role in more effective and specific cancer treatment. One of such targets is MTs and/or their major constituent subunits, tubulins. In cell division, during mitosis, MTs of the mitotic spindle are critical to the separation of chromosomes into two daughter cells [23, 24, 25]. Suppression of MT dynamics in cells by small molecule inhibitors blocks the cell division machinery at mitosis leading to cell death [27]. Therefore, the crucial role in cell division and in many other cellular events makes the MT system a well-validated target for the development of anticancer drugs [26]. This review is primarily focused on the role of MT/tubulin binding drugs as anti-cancer agents and recent development in this field.

Microtubule and Cell Cycle Progression

The fundamental task of the cell cycle is to produce two genetically identical cells from one (**Figure 1.1**). In order to accomplish this, the mother cell must replicate its

chromosomes exactly once during S-phase prior to entering mitosis, and at the end of mitosis each daughter cell must receive one and only one copy of each chromosome. To ensure this, the cell must precisely coordinate various complex events (**Figure 1.2**); one event must be prevented if proper completion of a preceding event is disrupted by physical damage or some other means. Cells in G1 have 1 copy of each chromosome or 2N DNA content. Cells that have completed DNA synthesis have 4N DNA content. S-phase is preceded by Gap-1 or G1 phase which allows the cell to grow and followed by Gap-2 or G2 phase which provides time for additional growth where the chromosomes condense, prior to mitosis. All these coordinated complex events during cell cycle division are mediated by cellular surveillance mechanisms called cell cycle checkpoints (**Figure 1.2**) (Mazia, 1961; Hartwell and Weinert, 1989; McIntosh, 1991) that monitor the completion of critical steps in the pathway. The metaphase-to-anaphase checkpoint inhibits the separation of sister chromatids until prerequisites for chromosome segregation have been satisfied (this is known as spindle checkpoint). The third mitotic checkpoint controls exit from mitosis (for example, if chromosomes did not divide properly). This is controlled by a Bub-2-dependent checkpoint that inhibits mitotic exit. The integrity and replication status of the genetic material before cells begin to replicate in S-phase is monitored by the START checkpoint. These conserved proteins such as p16, p21, and Rb ensure that the cell does not begin DNA replication unless the molecular machinery for DNA synthesis is ready. Drugs that block cell cycle progression by activating the checkpoint mechanisms are therefore very useful for chemotherapeutic treatment of various human cancers. In particular, certain chemical compounds that target microtubules of the mitotic spindle have proven effective for cancer treatment because they are able to arrest cell cycle progression at mitosis and ultimately lead to cell death.

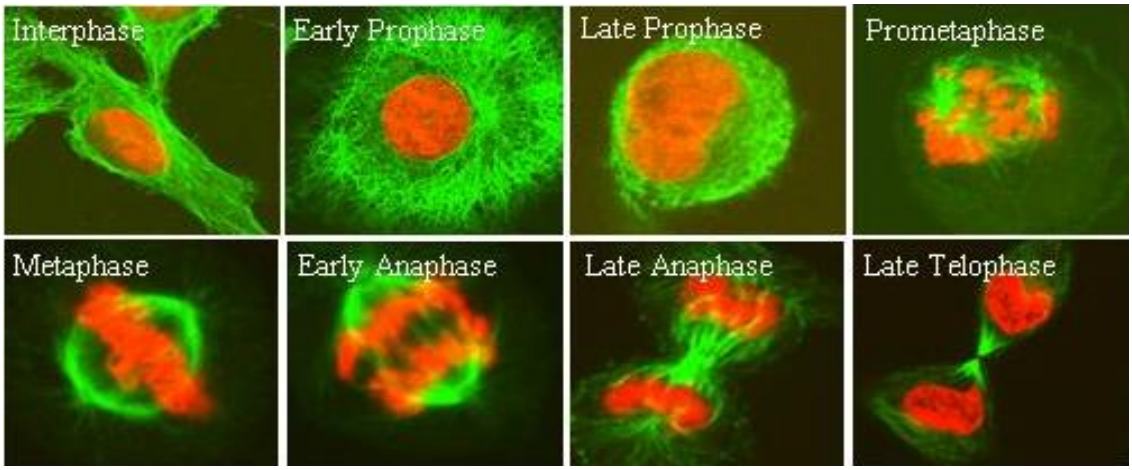

Figure 2. Demonstrates the different stages of mitosis cell division. Once chromosomes are aligned on the metaphase plate, cells wait until every one of the chromosomes is attached to the mitotic spindle before segregating chromosome to opposite poles, unless checkpoints are compromised such as in malignancies in which case cells end up becoming aneuploid, having one or more extra or fewer chromosomes than the normal 2N diploid and can potentially enter the next S-phase to become polyploid.

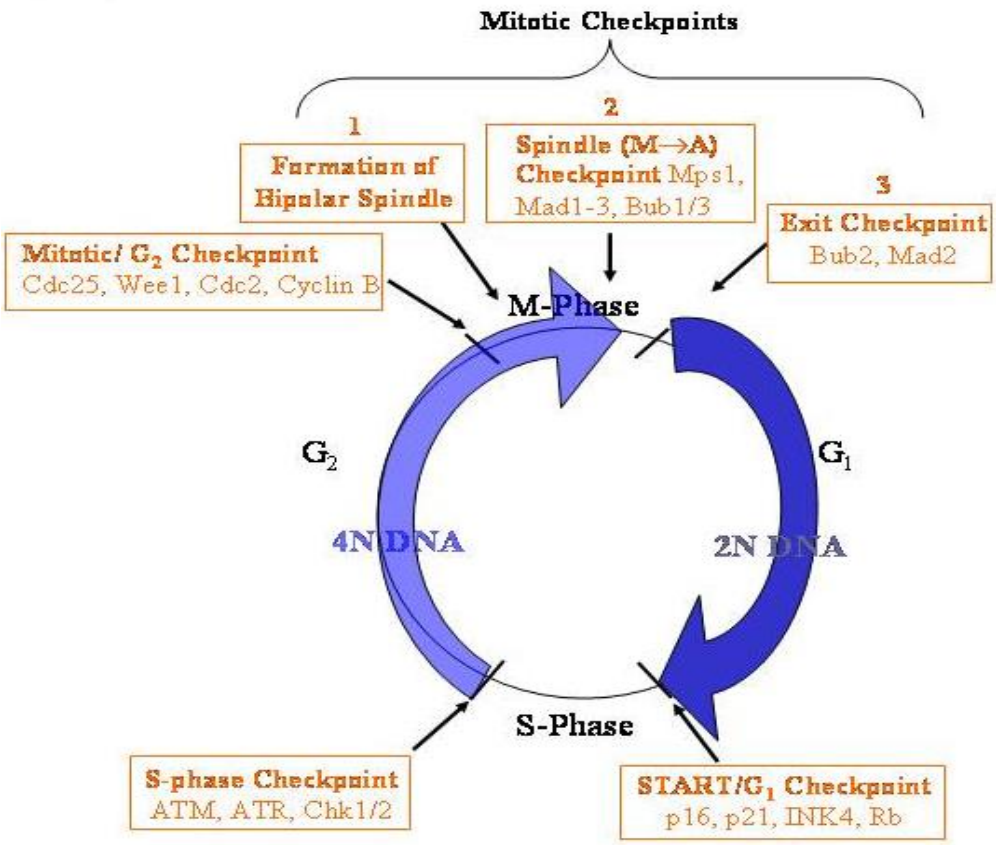

Figure 3. Demonstrating cell cycle progression and cell cycle checkpoints. Various steps of cell cycle progression are well coordinated by checkpoints that monitor the completion of critical steps in the pathway.

Mitosis and the Spindle Assembly Checkpoint

The spindle assembly checkpoint is a surveillance mechanism that ensures faithful transmission of chromosomes during mitosis; it examines whether prerequisites for chromosome segregation have been satisfied and thereby determines whether to execute or to delay chromosome segregation. The spindle assembly checkpoint is also known as the mitotic checkpoint (Li and Benezra, 1996), kinetochore attachment checkpoint (Rieder et al., 1994), chromosome distribution checkpoint (Nicklas, 1997), or simply the spindle checkpoint (Waters et al., 1998). At the heart of the spindle assembly checkpoint is the kinetochore, a multi-layered proteinaceous complex that assembles on the centromeric DNA of each chromosome (Rieder and Salmon, 1998). During mitosis, the kinetochore mediates the interaction between the chromosome and spindle microtubules. At the very beginning of prometaphase (i.e. immediately after the nuclear envelope breaks down), kinetochores are not attached to microtubules. Subsequently, one kinetochore on a chromosome captures microtubules from one spindle pole. When its sister kinetochore captures microtubules from the other pole, the now bioriented chromosome moves to the equatorial plane; this process is known as chromosome congression (Rieder and Salmon, 1994). Finally, all the chromosomes are attached through both kinetochores to microtubules from two opposite spindle poles and aligned at the equatorial plane, a stage referred to as metaphase. The spindle assembly checkpoint ensures that, only when all the chromosomes are properly attached and aligned at the equatorial plane, anaphase onset is triggered, allowing the splitting of sister chromatids and their delivery to each spindle pole (**Figure 1.3**).

The major components involved in the spindle assembly checkpoint were identified in two similar genetic screens in budding yeast for mutants that fail to arrest in mitosis in the presence of microtubule-interfering agents. These checkpoint components include Mad1, Mad2, Mad3 (mitotic arrest deficient, Li and Murray, 1991), Bub1 and Bub3 (budding uninhibited by benzimidazole, Hoyt et al., 1991). Subsequently, Mps1 (monopolar spindle 1) was also found to play a role in the spindle assembly checkpoint (Weiss and Winey, 1996). Over the past several years, homologs of many of these proteins have been

identified in mammalian cells (Li and Benezra, 1996; Taylor and Mckeon, 1997; Jin et al., 1998; Cahill et al., 1998; Taylor et al., 1998; Chan et al., 1998, 1999; Matinez-Exposito et al., 1999). The function of each of these checkpoint proteins is needed to prevent anaphase entry when the spindle has a defect or when chromosomes are not properly attached (Amon, 1999). Cells harboring mutations in these checkpoint genes proceed to anaphase prematurely and split sister chromatids regardless of whether the prerequisites for chromosome segregation have been satisfied. As a consequence, the delivery of exactly one copy of each chromosome to each daughter cell cannot be guaranteed, which can result in production of daughter cells that have gained or lost one or more chromosomes, a phenomenon termed aneuploidy (**Figure 1.3**). Missing or extra chromosomes in germ-line cells can result in premature abortion of the fetus or generation of offspring with birth defects such as Patau syndrome, Edwards syndrome, Down syndrome, and Klinefelter syndrome, which are characterized by the presence of an extra copy of chromosome 13, chromosome 18, chromosome 21, and X chromosome, respectively (Sluder and McCollum, 2000). Unequal chromosome segregation can also have severe consequences in adults by fostering tumor malignancy (Manchester, 1995). In fact, mutations in or reduced expressions of spindle assembly checkpoint components have recently been found in some types of human cancer (Li and Benezra, 1996; Cahill et al., 1998; Takahashi et al., 1999; Michel et al., 2001; Wang et al., 2002). For example, mutational inactivation of Bub1 has been implicated in human colorectal cancer (Cahill et al., 1998), and reduced expression of Mad2 has been implicated in human breast and ovarian cancers (Li and Benezra, 1996; Wang et al., 2002).

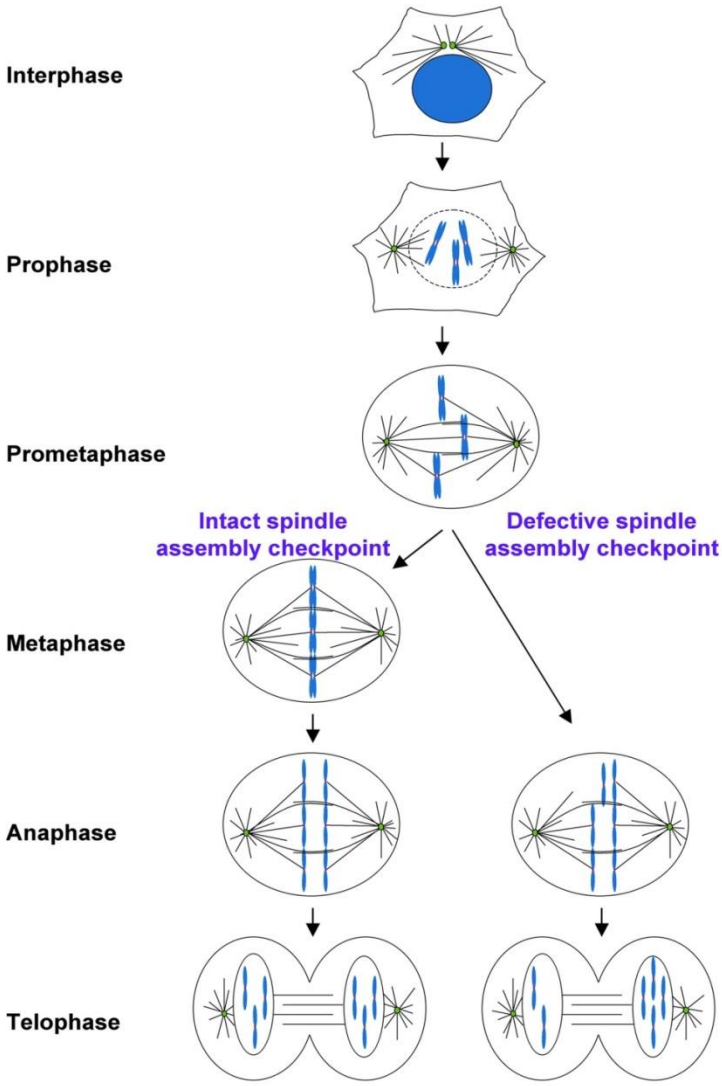

Figure 4. The spindle assembly checkpoint acts as a molecular safeguard in ensuring faithful chromosome transmission during mitosis. During prophase, the duplicated interphase chromatin condenses into chromosomes (blue) within the nucleus. Simultaneously, the radial array of microtubules (black lines) disappears, and a bipolar array (the mitotic spindle) forms by microtubules emanating from two opposite poles (green) defined by the previously duplicated and now separated pair of centrosomes. Subsequently, the nuclear envelope breaks downs marking the initiation of prometaphase. During this stage, the kinetochores (red) on chromosomes encounter and capture spindle microtubules. When a chromosome becomes attached by microtubules from two opposite spindle poles, it congresses to the equatorial plane (the metaphase plate). In the presence of intact spindle assembly checkpoint, anaphase onset is triggered when and only when all the chromosomes are attached through kinetochores by microtubules from two spindle poles and correctly aligned at the equatorial plane, a stage referred to as metaphase. However, in cells that have defective spindle assembly checkpoint, anaphase onset is triggered prematurely despite the presence of unattached or improperly attached chromosomes, resulting in missing or extra chromosomes (aneuploidy) in the daughter cells.

Microtubule Structure and Dynamics

Microtubules (MTs) are major dynamic structural components in cells. They are important in the development and maintenance of cell shape, in cell reproduction and division, in cell signaling, intracellular transport of vesicles and organelles and in cellular movement (Lodish et al., 1999). During cell division, MTs form a bipolar apparatus, called the mitotic spindle *responsible for the accurate distribution of chromosomes into two daughter cells*. Microtubules are composed of 13 protofilaments in most cells, align laterally and give rise to hollow, helical cylindrical structure of 25 nm diameter that may be many μm long (Figure 1.4). Each protofilament is assembled from head-to-tail arrangement of two similar but non-identical subunits referred to as α-tubulin and β-tubulin (Amos and Klug, 1974), which are about 50% identical at the amino acid level (Burns, 1991). The □-tubulin monomer was found to be composed of 451 amino acid residues and the □-tubulin monomer consisted of 445 amino acid residues. The α- and β-tubulin monomer each has a molecular mass of about 50 kDa and each binds a guanosine triphosphate (GTP) molecule (Weisenberg et al., 1968), nonexchangeable in α-tubulin and exchangeable in β-tubulin (Spiegelman et al., 1977). The head-to-tail association of tubulin dimer gives microtubules an intrinsic polarity in their structure. One end of the microtubule is capped with α-tubulin while the other end is capped with β-tubulin (Mandelkow et al., 1986; Song and Mandelkow, 1995; Fan et al., 1996a). The structural polarity of the microtubule influences the dynamic property of its two ends. One end, called the plus end that grows and shortens much faster than the other end, called the minus end (Allen and Borisy, 1974). The three dimensional structure of the tubulin heterodimer was obtained by electron crystallography studies (Figure 1.5). Each monomer is asymmetric with approximate dimensions of 46 × 40 × 65 Å (width, height and depth, respectively) and consists of a core of two sheets surrounded by helices (Nogales et al., 1999). Functionally each subunit of tubulin is divided into three domains: the amino terminal domain containing the nucleotide binding region, an intermediate domain and the carboxyl terminal domain that regulate the interaction of drugs such as vinblastine and colchicine (Rai et al., 1998; Chakraborty et al., 2004).

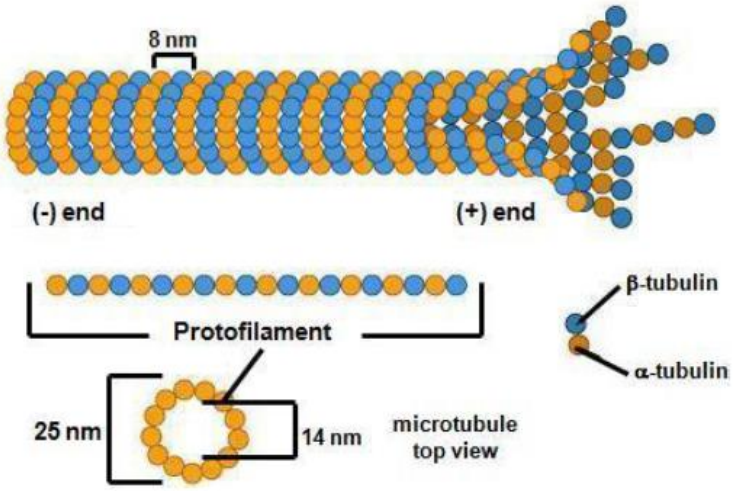

Figure 5. Schematics showing the structure of microtubule. They are hollow tube like structures formed from oligomeric structures known as protofilaments. The protofilaments contain repeating units of α- and β-tubulin heterodimers that are assembled exclusively onto the plus (+) end of the microtubule (adapted from Moore, 2008. Manual of Cellular and Molecular Functions).

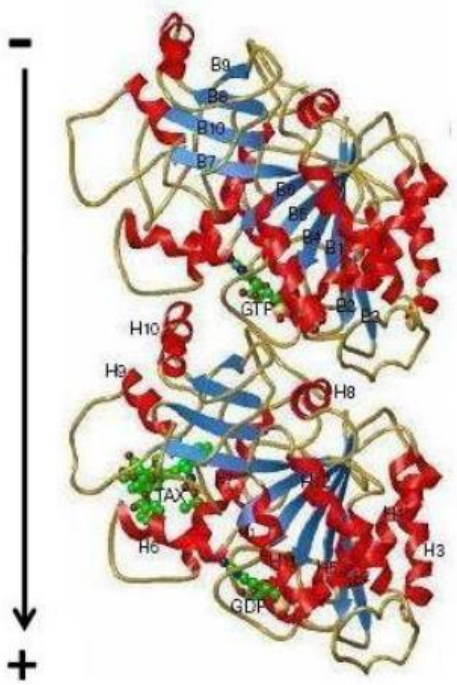

Figure 6. Ribbon diagram showing the α- and β-monomers of tubulin from X-ray crystallographic data at a resolution of 3.7 Å viewed from inside of the microtubules. The tubulin consisted of alpha helix, beta strands and loops. The GTP (non-hydrolyzable) is shown to bind to the α-monomer whereas GDP (formed from the hydrolysis of GTP, hydrolyzabe site of GTP) and Taxotere are bound to β-monomer. Colchicine bound at the interface between α- and β- tubulin. The arrow indicates the growth of the protofilaments during microtubule formation (Nogales et al., 1998).

Microtubules are intrinsically dynamic polymers (Margolis and Wilson, 1978; Mitchison and Kirschner, 1984a, b; Saxton et al., 1984; Schulze and Kirschner, 1986; Belmont et al., 1990), and they grow and shorten by the reversible noncovalent addition and loss of tubulin dimer at their ends. GTP binds to free tubulin in an exchangeable fashion and becomes irreversibly hydrolyzed to guanosine diphosphate (GDP) during the

addition of tubulin dimer to the ends of microtubules (David-Pfeuty et al., 1977; MacNeal and Purich, 1978). This gives rise to two unusual dynamic behaviors. Dynamic instability describes the abrupt and stochastic alternation of microtubules between periods of growth and shortening (Mitchison and Kirschner, 1984a, b), and treadmilling describes the net growth of microtubules at one end and the net shortening at the other end (Margolis and Wilson, 1978). Several parameters have been used to characterize the dynamics of microtubule assembly (Walker et al., 1988; Jordan and Wilson, 1999). These include growth rate, shortening rate, frequency of transitions from growth to shortening (catastrophe frequency), frequency of transition from shortening to growth or an attenuated (pause) state (rescue frequency), and the duration of the attenuated state when neither microtubule growth nor shortening can be detected (**Figure 1.6**). Overall microtubule dynamics due to dynamic instability is described as dynamicity, which measures the sum of visually detectable tubulin dimer exchange per unit time at the ends of microtubules (Jordan and Wilson, 1999). The dynamic property is crucial for microtubules to carry out many of their cellular functions such as reorientation of the microtubule network when cells undergo migration or morphological changes and the dramatic microtubule rearrangement at the onset of mitosis (Joshi, 1998). Mitotic microtubules are 10-100 times more dynamic than interphase microtubules; they exchange their tubulin with the soluble tubulin pool with half-times of ~15 s during mitosis as compared with 3 min to several hours in interphase (Saxton et al., 1984; Schulze and Kirschner, 1986; Belmont et al., 1990). The rapid microtubule dynamics in mitosis is thought to be critical for both the morphogenesis and activities of the mitotic spindle that directs chromosome congression to the equatorial plane (also called the metaphase plate) and their final segregation into the daughter cells.

Mitotic Arrest and Apoptosis

Typically, cells treated with microtubule-interfering agents arrest at mitosis, resulting from the disruption of spindle functions, and then undergo death (Dustin, 1984). It had therefore been thought that the antitumor activity of microtubule-interfering agents is a consequence of blocking mitotic progression (Milas et al., 1995;

Wahl et al., 1996), and the subsequent cell death is a consequence of a catastrophic resolution of the abnormal mitosis, termed mitotic catastrophe (Russel and Nurse, 1986, 1987; Heald et al., 1993). Several lines of compelling evidence suggest that microtubule-interfering agents are able to induce both morphological and biochemical features of typical apoptosis, including chromatin condensation, cell membrane blebbing, and internucleosomal DNA fragmentation (Bhalla et al., 1993; Bonfoco et al., 1995; Woods et al., 1995; Kawamura et al., 1996; Jordan et al., 1996). These results indicated that microtubule-interfering agents, in addition to blocking mitosis, could induce apoptotic pathways in many types of cells. The next question was whether the mitotic arrest and apoptosis caused by microtubule-interfering agents were two intimately related events or two independent consequences of disrupting the normal physiological balance of microtubule dynamics. Because mitotic arrest caused by antimicrotubule agents precedes apoptosis, a natural hypothesis that mitotic arrest was the cause of apoptosis has gained widespread support (King and Cidlowski, 1995).

However, several recent studies suggest that microtubule-interfering agents might induce apoptosis via signaling pathways independent of mitosis (Long and Fairchild, 1994; Fan et al., 1996b; Lieu et al., 1997; Fan et al., 1998; Miller et al., 1999). For example, either a brief exposure to a high concentration of paclitaxel or a long exposure to a low concentration of paclitaxel could drive cells into apoptosis in the absence of mitotic block (Long and Fairchild, 1994; Lieu et al., 1997). In addition, baccatin III, the central ring system of paclitaxel structure, has been found to induce apoptotic cell death without causing mitotic arrest; instead, many apoptotic events were found in other phases of the cell cycle (Fan et al., 1998; Miller et al., 1999). Another significant evidence that supports the apoptotic pathway independent of mitotic arrest comes from the finding that glucocorticoids selectively inhibit paclitaxel-induced apoptosis without blocking cells at mitotis (Fan et al., 1996b). Thus, the precise molecular mechanisms underlying apoptosis and mitotic arrest induced by antimicrotubule agents and the relationship between the two events are not clear at present.

The ability of microtubule-interfering agents to arrest mitosis and induce apoptosis provides a molecular basis for their use in chemotherapeutic treatment of human cancers. Microtubule drugs currently in clinical use for cancer chemotherapy include paclitaxel, docetaxel, and the vinca alkaloids. Specifically, paclitaxel has proven effective against refractory ovarian cancer, metastatic breast cancer, and non-small-cell lung cancer (Rowinsky, 1997; Crown and O'Leary, 2000), and the vinca alkaloids are effective against cancer types such as lymphoma, leukemia, and Kaposi's sarcoma (van Tellingen et al., 1992). Unfortunately, the toxicity and low aqueous solubility have limited the applicability of the taxoids and vinca alkaloids in cancer chemotherapy. Moreover, their use has been hampered by the development of drug resistance contributed by multifactorial mechanisms, such as overexpression of P-glycoprotein (Gottesman and Pastan, 1993; Bradley and Ling, 1994), altered expression of tubulin isotypes (Burkhart et al., 2001), and the presence of tubulin mutations (Giannakakou et al., 1997). Therefore, development and/or discovery of microtubule-based compounds are in demand, especially for the treatment of human cancers resistant to currently used drugs.

Noscapine: a Plant Derived Alkaloid

Noscapine was originally discovered by French pharmacist and Professor Pierre-Jean Robiquet in 1817. He isolated two natural compounds from opium (Papaver somniferum): codeine and noscapine (Warolin et al., 1999) (Figure 1.8). Noscapine (21%) is one of the more abundant opium alkaloids, the other prominent alkaloids being morphine (42%), codeine (12%), papaverine (18%), thebaine (6.5%) sanguinarine, berberine and tubocurarine. The pioneering step has been achieved by Perkin and Robinson (1910), who could obtain noscapine from meconine and cotarnine in the presence of potassium carbonate combined with fractional crystallization. Since then, tremendous progress has been made in the development of schemes for total synthesis. However, the availability of noscapine from natural sources is perhaps more economical than the current synthetic means. The elucidation of novel and simpler synthetic methods will continue to provide further synthesis of novel derivatives. Traditionally, a mode of combinatorial chemistry

(A) *Opium (poppy)*

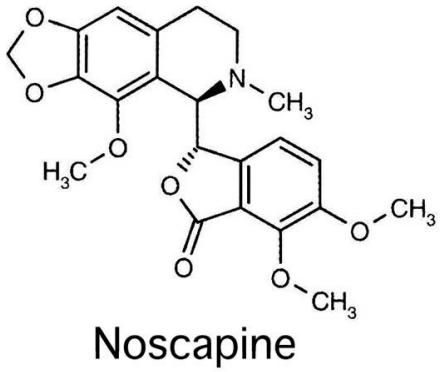

Noscapine

Figure 7. The opium poppy and the chemical structure of its alkaloid, Noscapine.

has been of immense value in drug development. Noscapine however, faces a bit of a challenge because of the linkage between the two ring systems i.e. the iso-quinoline ring and the iso-benzo-furanone ring system are joined by a single rotatable c-c bond involving two chiral centers. This necessarily leads to a racemic mixture of 4-stereoisomers of noscapine in ordinary chemical reactions. Only one of these stereoisomers, the RS form is active biologically (Ye et al., 1998; Karlsson et al., 1990). Nevertheless the improvements in the separation techniques of the chiral molecules as well as innovations in the chirally biased synthetic procedures may capitalize on the combinatorial potential of novel synthesis. In addition, many natural compounds such as taxanes can be easily synthesized starting from a natural derived core structure system in a more economical fashion (Nicolaou et al., 1994), similar principles might also apply to noscapine.

Discovery of Noscapine as a New Anti-microtubule Drug

Noscapine is a non-narcotic, phthalide isoquinoline alkaloid derived from the opium poppy Papaver somniferum. It has been used since long time as a cough suppressant in humans and in experimental animals (Chopra et al., 1930; Winter and Flataker, 1954; Empey et al., 1979; Dahlstrom et al., 1982; Karlsson et al., 1990). During a systematic screen based on structural similarity of known drugs that interfere with microtubules, Ye et al. (1998) have identified the opium alkaloid noscapine as a novel microtubule-interfering agent. Noscapine acts mechanistically similar to many other microtubule agents, in that it binds stoichiometrically to the tubulin subunits of microtubules, with one noscapine

molecule per tubulin dimer, and alters the conformation of tubulin upon binding (Ye et al., 1998). Presence of noscapine does not promote or inhibit MT polymerization in vitro unlike Paclitaxel and Nocodazole. Instead, noscapine alters the steady state dynamics of MT assembly, primarily by increasing the amount of time that MTs spend in an attenuated (pause) state (**Figure 1.10**).

Noscapine Possesses Low Cytotoxicity Activity to Cancer Cells

The cytotoxicity activity of noscapine to cancer cells of various tissue origins was evaluated previously by the National Cancer Institute (NCI) through its Developmental Therapeutic Program (DTP) against their panel of 60 human cancer cell lines. The panel of 60 human tumor cell lines is organized into subpanels representing leukemia, non-small cell lung, colon, central nervous system (CNS), melanoma, renal, ovarian, breast and prostate cancer lines. **Table 1.1** included the IC_{50} values of noscapine towards various cancer cell lines— the IC_{50} values remain in the high micromolar ranges (~21.1 to 100 μM) (Ye et al., 1998).

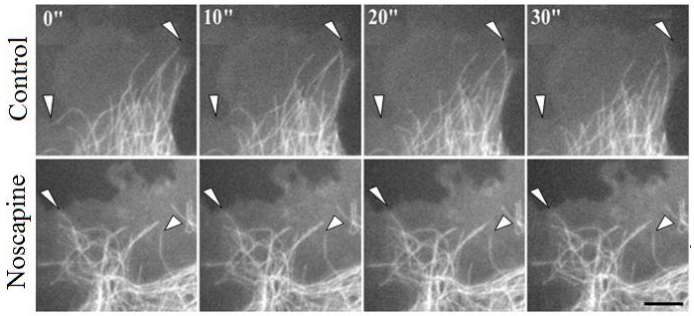

Dynamic Parameters	Control	Noscapine 25µM	Noscapine 250µm
	37 MTs	45 MTs	44 MTs
Growth	n=96	n=89	n=14
Rate (µm/min)	9.89 ±0.78	9.29 ±1.05	6.34 ±0.72
Distance (mm)	1.16 ±0.09	0.97 ±0.10	0.75 ±0.03*
Duration (sec)	9.62 ±0.95	8.30 ±1.44	8.04 ±0.74
Shrink	n=78	n=79	n=19
Rate (µm/min)	11.39 ±0.81	9.06 ±0.76*	8.89 ±1.19*
Distance (mm)	1.60 ±0.30	1.04 ±0.09	1.26 ±0.36
Duration (sec)	8.75 ±1.26	8.06 ±0.58	9.62 ±2.13
Average Pause Duration (sec)	n=109 22.54 ±2.18	n=132 34.66 ±3.27*	n=68 77.60 ±5.68*
% Time per Phase Growth/Shrink/Pause	22.7/16.8/60.5	12.3/10.8/76.9	2.0/3.3/94.7
Rescue Frequency (sec^{-1})	0.147 ±0.02	0.128 ±0.01	0.138 ±0.03
Catastrophe Frequency (sec^{-1})	0.029 ±0.004	0.028 ±0.004	0.007 ±0.001*
Dynamicity (µm/min)	102.70 ±12.94	57.50±7.72*	10.40 ±2.83*

Figure 8: A gallery of video frames, 10 seconds apart, showing the plus ends of several microtubules in a control and a noscapine-treated mammalian rat kangaroo endothelial PtK2 cells. Quantitative parameters of microtubule dynamics are listed in table. Values are mean + SEM. Noscapine increases the average time cellular microtubules remain inactive (pause duration) (Ye et al., 1998).

(a) Leukemia cell line	IC_{50} (μM)	(b) CNS cancer	IC_{50} (μM)	(c) Colon cancer	IC_{50} (μM)	(d) Ovarian cancer	IC_{50} (μM)
HL-60(TB)	26.4	SF-268	71.7	COLO205	63.6	IGROV1	62.6
K-562	33	SF-295	30.2	HCC2998	79.5	OVCAR-3	16.5
MOLT-4	23.5	SF-539	30.7	HCT-116	50.5	OVCAR-4	100
RPMI-8226	23.3	SNB-19	80.5	HCT-15	43.3	OVCAR-5	100
SR	38.9	SNB-75	4.87	HT29	40	OVCAR-8	63.5
CCRF-CEM	12.9	U251	41	KM12	45.8	ADR-RES	43.8
				SW-620	27	SK-OV-3	73.1
(e) Melanoma	IC_{50} (μM)	(f) Non-small lung ca	IC_{50} (μM)	(g) Breast cancer	IC_{50} (μM)	(h) Renal cancer	IC_{50} (μM)
LOX IMVI	37.2	A549	72.9	MCF7	42.3	786-0	49.9
MALME-3M	33.5	EKVX	100	MDA-MB-231	76.5	A498	100
M14	39.2	HOP-62	71.4	HS 578T	21.1	ACHN	62.6
MDA-MB-435	4.86	HOP-92	100	BT-549	45.7	CAKI-1	63
SK-MEL-2	34.1	H226	100	T-47D	100	RXF 393	100
SK-MEL-28	42.1	H23	79.1	MDA-N	23.1	SN12C	100
SK-MEL-5	48.3	H322M	100	(i) Prostate cancer	IC_{50} (μM)	TK-10	100
UACC-257	55	H460	39.9	PC-3	50.1	UO-31	69.1
UACC-62	56.9	H522	30.3	DU-145	100		

Table 1. NCI 60 cell lines screening of Noscapine. From the various cell lines screening, it was found that many cell lines tested were inhibited by the presence of noscapine to various extents.

Noscapinoids: the Synthetic Analogues of Noscapine

To enhance the cytotoxicity activity of noscapine a battery of analogues were design and chemically synthesized previously (collectively called as noscapinoids) as included in **Figure 1.15** and **1.16** (Aggarwal et al., 2002; Aneja et al., 2006a; Aneja et al., 2006b; Aneja et al., 2006c). Some of these derivatives (mostly the halogen derivatives, **Figure 1.16**) have much better therapeutic indices and improved pharmacological profiles. As an example the effectiveness of noscapine was improved by synthesizing many potent noscapine derivatives with increasing tubulin binding affinity by decreasing the dissociation constant (K_d) between tubulin-drug complex from 144 μM to 86 μM by nitro-noscapine, 80 μM by F-noscapine, 54 μM by Br-noscapine, 40 μM by Cl-noscapine, and 22 μM by I-noscapine (Aneja et al., 2006a; Aneja et al., 2006b).

Scheme 1. Semi-synthetic derivatives of noscapine[a]

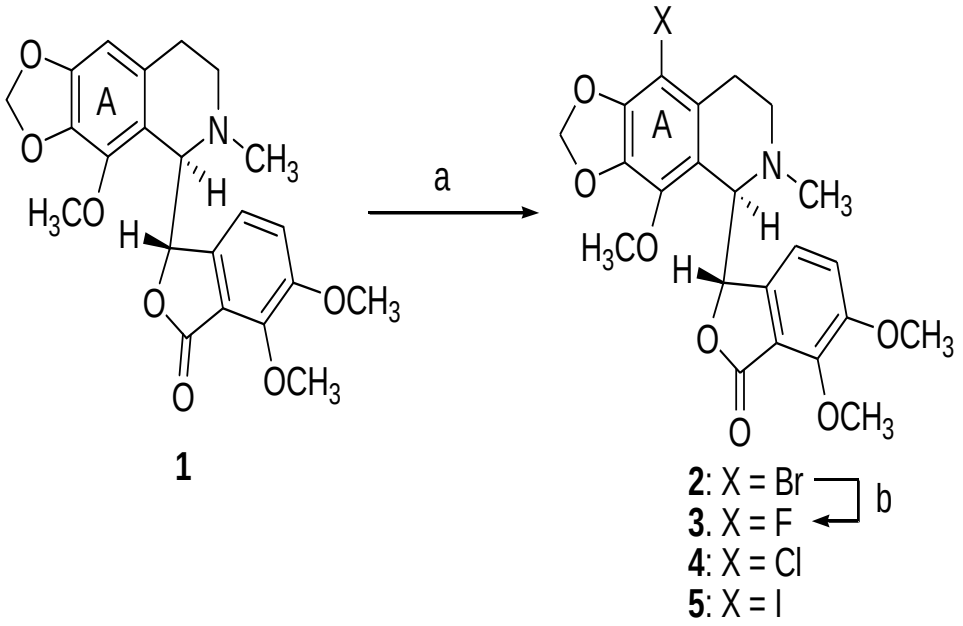

[a]Reagents and reaction conditions. a) compound **2**. Br_2-H_2O, 48% HBr, 82%; compound **4**. SO_2Cl_2, $CHCl_3$, 90%; compound **5**. Pyr-ICl, CH_3CN, 71%; b) F_2, Amberlyst-A, THF, 74%.

Figure 9. Halogenated derivatives of noscapine.

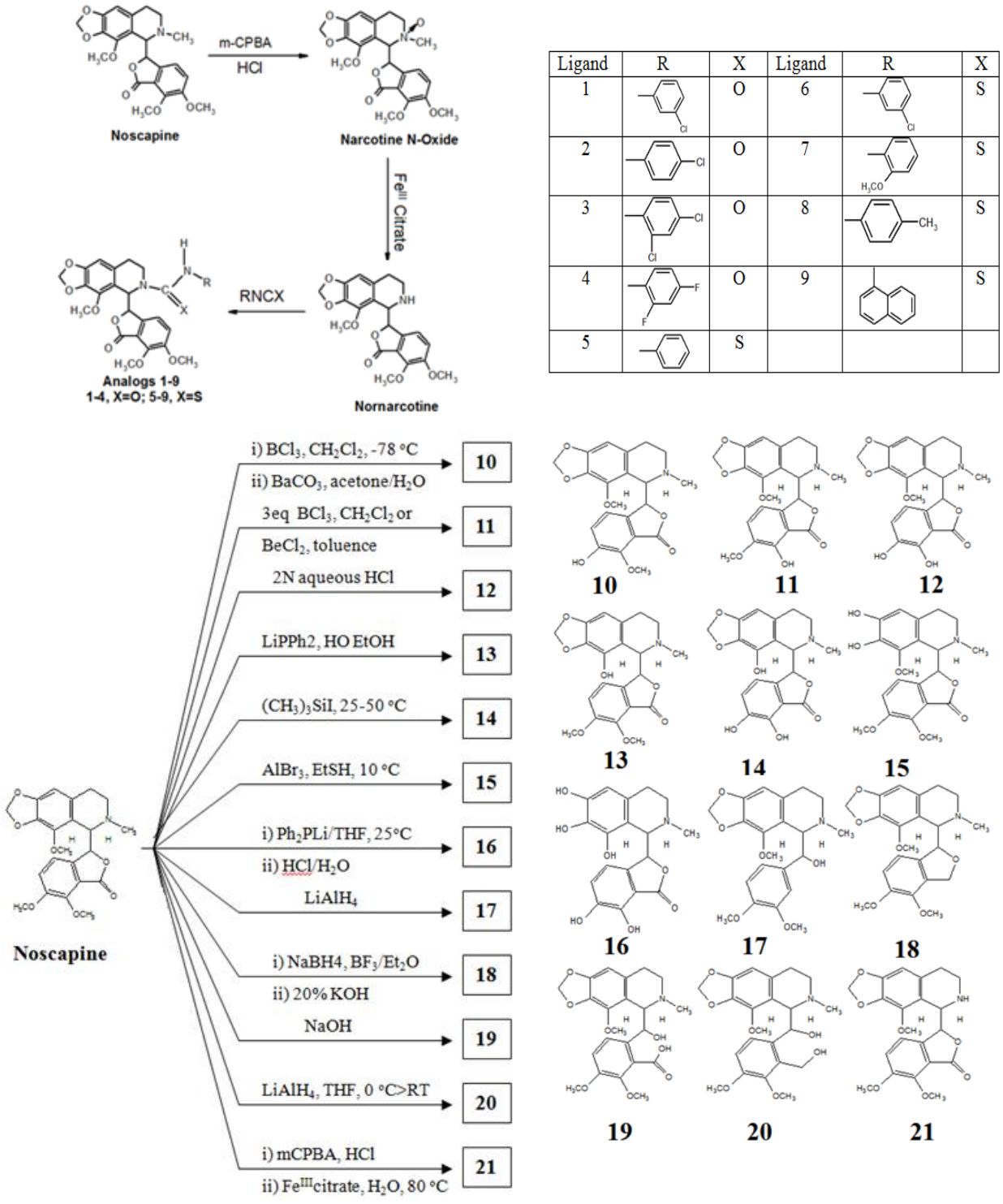

Ligand	R	X	Ligand	R	X
1		O	6		S
2		O	7		S
3		O	8		S
4		O	9		S
5		S			

Figure 10. Aryl-derivatives of noscapine. These derivatives were synthesized by functionalization by deleting or substitution of various functional groups as mentioned in the noscapine scaffold. All these derivatives showed very little or no improvement in cytotoxicity activity of noscapine.

It is noteworthy that noscapinoids cause no histopathological, hematological, immunological and neuronal toxicity at concentrations as high as 300 mg/kg. Many of these noscapine derivatives have been shown previously to inhibit cellular proliferation of a wide variety of cancer cells (panel of NCI 60 cancer cell lines) including many drug-resistant variants while evading normal cells. In addition they effectively regress human tumor xenografts (lymphomas, breast, prostate and melanomas) implanted in preclinical mice models to a fair degree. However, a complete elimination of the disease was not achieved even on increasing dosages as high as 600 mg/kg. Therefore attempts should be made to design new generation of noscapine derivatives for the better therapeutic outcome.

Computer-aided Design of Potent and Novel Noscapine Analogues

Drug discovery and development is a time-consuming and expensive process. On average, it takes 10–15 years and US $500–800 million to introduce a drug into the market (Workman, 2003; Brown and Superti-Furga, 2003). This is why computer-assisted drug design (CADD) approaches have been widely used in the pharmaceutical industry to improve the efficiency of the drug discovery and development pipeline (Gomeni et al., 2001; Veselovsky and Ivanov, 2003). CADD helps scientists focus on the most promising compounds so that they can minimize the synthetic and biological testing efforts. To identify and design small molecules as clinically effective therapeutics, various computational methods have been evaluated as promising strategies, depending on the purpose and systems of interest. In practice, the choice of CADD approaches to be employed is usually determined by the availability of the experimentally determined 3D structures of target proteins. If protein structures are unknown, various methods of ligand-based drug design can be employed, such as Quantitative Structure Activity Relationship (QSAR) and pharmacophore analysis. If the target structures are known, structure-based approaches can be used such as molecular docking, which employs the target 3D structures to design novel active compounds with improved potency. As more structures are becoming available, the prediction accuracy will likely to be improved. These state-of-the-art tools have been used for the discovery and development of active agents for various diseases, in particular for cancer therapies.

Availability of structure activity data of many derivatives of noscapine leads to develop a reasonable theoretical prediction model and thus guided in rational design of more potent derivatives of noscapine. Theoretical calculations, in particular the molecular docking method seems to be a primary tool for gaining such understanding. The docking algorithms provide good-quality binding pose for a compound that fits into the binding cavity of target receptor and evaluates its binding affinity using scoring function. However, the scoring functions used by docking algorithms are very simple. They generally do not include shape complementarity parameters between binding cavity and the ligand as well as the solvation effect in calculating the electrostatic interactions energy between protein and ligand. Thus using of molecular docking only in designing or screening of ligands may be problematic and can result in a decrease of accuracy. To overcome the problem in molecular docking, more precise but time consuming computational methodologies are necessary to rescore the docking results. This inspired me to use molecular mechanics in combination with generalized Born solvation area (GBSA) in calculating the binding affinity between protein and ligands.

Chapter-3

Objective

To design novel derivatives of noscapine (we called as fourth generation) using structure based computer aided molecular designing techniques. First a library of noscapine derivatives will be developed by substituting various functional groups in the scaffold structure using combinatorial chemistry. The potent derivatives with improved binding affinity onto tubulin will be screened out based on molecular docking and MM-GBSA. Moreover their binding mode with tubulin will be elucidated.

Materials and methods

Ligand Preparation

Molecular structures of novel derivatives of noscapine 4**a-m** (**Figure 11**) were built using molecular builder of Maestro (version 9.2, Schrödinger). All these structures were energy minimized using Macromodel (version 9.9, Schrödinger) and OPLS 2005 force field with PRCG algorithm (1000 steps of minimization and energy gradient of 0.001). Appropriate bond order for each structure was assigned using Ligprep (version 2.5, Schrödinger). Complete geometrical optimization of these structures was carried out using hybrid density functional theory with Becke's three-parameter exchange potential and the Lee-Yang-Parr correlation functional (B3LYP) (Lee et al., 1988; Becke, 1993) using basis set 3-21G* (Binkley et al., 1980; Gordon et al., 1982; Pietro et al., 1982). Jaguar (version 7.7, Schrödinger, LLC) was used for the geometrical optimization of the ligands.

Protein Preparation

The co-crystallized podophyllotoxin-tubulin complex structure (PDB ID: 1SA1, resolution 3.58Å) was used for molecular docking and rescoring. Multi-step Schrödinger's protein preparation wizard (PPrep) was used for the final preparation of protein. Missing hydrogen atoms were added to the structure using Maestro interface (version 9.2, Schrödinger). All the water molecules were removed from the complex and the hydrogen bond network was optimized using PPrep wizard. The missing amino acids from 37 to 47 (A-chain) and 275 to 284 (B-chain) in the co-crystallized structure were filled using homology-based modeling technique based on different templates such as PDB ID: 3DU7 (C-chain) and PDB ID: 3RYC (D-chain) respectively, using Prime (version 3.0, Schrödinger). The structure obtained was energy minimized using OPLS 2005 force field with Polak-Ribiere Conjugate Gradient (PRCG) algorithm. The minimization was stopped either after 5,000 steps or after the energy gradient converged below 0.001 kcal/mol. All atom molecular dynamics (MD) simulation of protein structure in explicit water was carried out using the GROMACS 4.5.4 software (Berendsen et al., 1995) and the GROMOS96 force field for a time scale of 10 ns. Three-dimensional periodic boundary conditions were imposed, enclosing the molecule in a dodecahedron solvated with the SPC216 water model provided in the GROMACS package and energy minimized using 1000 steps of steepest descent. The system was neutralized with 32 Na^+ counterion and was locally minimized using 100 steps of steepest descent. The electrostatic term was described using the Particle Mesh Ewald algorithm (Daren et al., 1993). The LINCS (Hess et al., 1997) algorithm was used to constrain all bond lengths and cut-off distances for the calculation of the coulombic and van der Waals interactions at 1.0 nm. The system was equilibrated by 100 ps of MD runs

with position restraints on the protein to allow the relaxation of the solvent molecules at 300 K and normal pressure. The system was coupled to the external bath by the Berendsen thermostat with a coupling time of 0.1 ps with default setting. The final MD calculations were performed for 10.0 ns under the same conditions, except the position restraints. The overall quality of the model, stereochemical values and non-bonded interactions were tested using PROCHECK (Laskowski et al., 1993), ERRAT (Colovos and Yeates, 1993) and VERIFY3D (Eisenberg et al., 1997). The PROCHECK results showed 94.8% of backbone angles are in allowed regions with G-factors of -0.12. Ramachandran plot (Ramachandran et al., 1963) analysis revealed only 1.6% residues in the disallowed region and 2.3% residues in generously allowed regions. ERRAT is an "overall quality factor" calculator program for non-bonded atomic interactions. The accepted range in ERRAT is 50 and higher scores indicate the precision of the model. In the case of tubulin, the ERRAT scores was 88.402 that is within the range of high quality model. Similarly, the VERIFY 3D score of 95.25% indicates a good quality model.

Molecular Docking of Ligands and Calculation of Binding Free Energies

The receptor-grid file was generated at the centroid of the noscapinoid binding site (Naik et al., 2011) using Glide (version 5.7, Schrödinger). A bounding box of size 12Å x 12Å x 12Å was defined in tubulin and centered on the mass center of binding site in order to confine the mass center of the docked ligand. The larger enclosing box of size 12Å x 12Å x 12Å which occupied all the atoms of the docked poses was also defined. The scale factor of 0.4 for van der Waals radii was applied to atoms of protein with absolute partial charges less than or equal to 0.25. All the ligands were then docked into the binding site using

Glide XP (extra precision) and evaluated using a Glide XP_{Score} function (Friesner et al., 2004; Halgren et al., 2004).

Rescoring using Prime/MM-GBSA approach

For each ligand, the pose with the lowest Glide score was rescored using Prime/MM-GBSA approach (Lyne et al., 2006). This approach is used to predict the free energy of binding for set of ligands to receptor. The docked poses were minimized using the local optimization feature in Prime and the energies of complex were calculated using the OPLS-AA force field and generalized-Born/surface area (GBSA) continuum solvent model. The binding free energy (ΔG_{bind}) is then estimated using equation:

$$\Delta G_{bind} = E_{R:L} - (E_R + E_L) + \Delta G_{solv} + \Delta G_{SA} \qquad (1)$$

where $E_{R:L}$ is energy of the complex, $E_R + E_L$ is sum of the energies of the ligand and unliganded receptor, using the OPLS-AA force field, ΔG_{solv} (ΔG_{SA}) is the difference between GBSA solvation energy (surface area energy) of complex and sum of the corresponding energies for the ligand and unliganded protein. Corrections for entropic changes were not applied in this type of free energy calculation.

Results and discussion

Validation of docking methods

The original crystal structure of tubuline-podophyllotoxin complex (PDB ID: 1SA1) was used to validate the Glide-XP docking protocol. This was done by moving the co-crystallized podophyllotoxin ligand outside of active site and then docking it back into the active site. The top 10 configurations after docking were taken into consideration to validate the result (Table 2). The RMSD was calculated for each configuration in comparison to the co-crystallized podophyllotoxin and the value was found to be in between 0.02-0.85 Å.

Table 2. The RMSD and docking score from the docking simulation of 10 lowest configurations of co-crystal podophyllotoxin in Tubulin protein (ISA1).

Configuration	Glide Score	[a]ΔG_{score}	[b]RMSD (Å)	[c]RMSD (Å)
1	-10.26	0	0.85	0.60
2	-10.20	-0.06	0.02	0.86
3	-9.80	-0.46	0.68	1.33
4	-9.72	-0.54	0.57	1.26
5	-9.50	-0.76	0.04	0.67
6	-9.25	-1.01	0.04	0.67
7	-8.78	-1.48	0.80	0.59
8	-8.47	-1.79	0.13	1.02
9	-7.87	-2.39	0.03	0.79
10	-7.72	-2.54	0.07	0.90

[a]ΔG_{score} = E_i-$E_{lowest;}$ [b]RMSD = RMSD between docked and crystallographic podophyllotoxin structure; [c]RMSD = RMSD between docked poses corresponding to each configuration.

Whereas the RMSD value calculated out of 10 accepted poses for each configuration was found in between 0.59 – 1.33 Å. This revealed that the docked configurations have similar binding positions and orientations within the binding site and are similar to the crystal structure. The best docked structures, which is the configuration with the lowest Glide score is compared with the crystal structure as shown in Figure 11(a-b). These docking results illustrate that the best-docked podophyllotoxin complex agrees well with its crystal structure and that Glide (XP)-docking protocol successfully reproduces the crystal tubulin-podophyllotoxin complex.

Glide 4.0 in XP mode have been used to dock the newly designed noscapinoid derivatives onto the noscapinoid binding site of tubulin. The binding mode of these derivatives within noscapinoid binding is represented in Figure 12a-c. In this figure we can observe that all the ligands are well fitted to the defined binding pocket. All the 18 noscapinoids were found to be good binder with tubulin. Table 3 reveals the Glide score and other relevant parameters of noscapinoids. The details of hydrogen bonding and hydrophobic contribution of binding site amino acids with the noscapinoids are included in the ligplot (Figure 13).

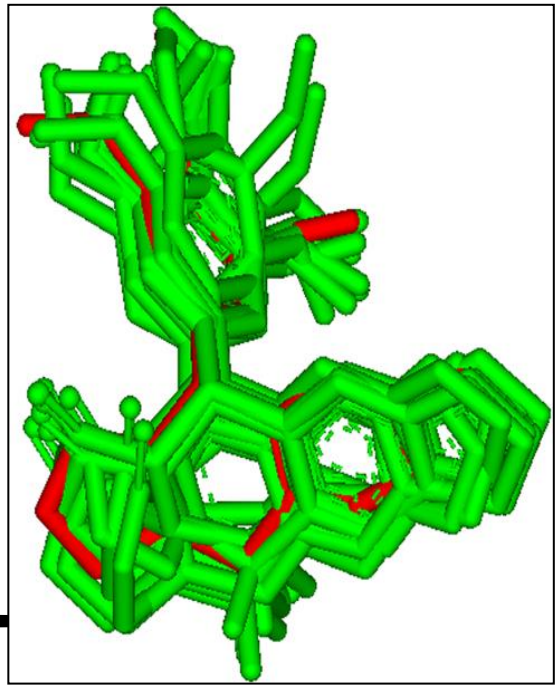

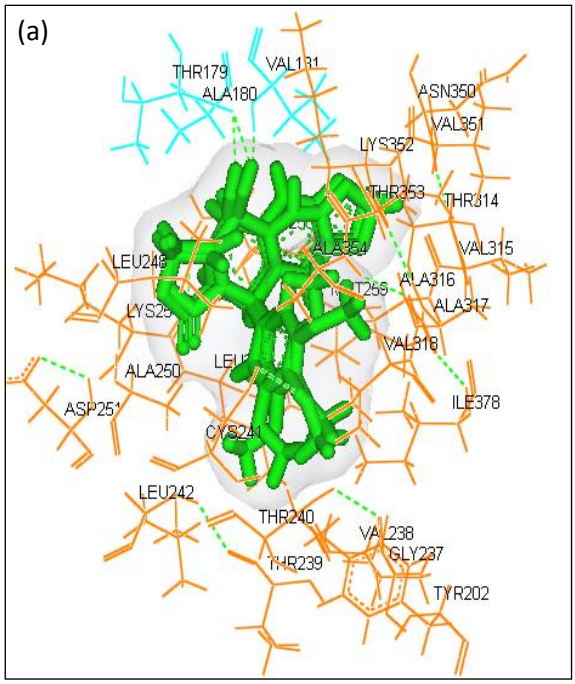

Figure 11. Superposition of the docked configurations of co-crystallized podophyllotoxin: (a) with binding site and (b) only the superposed structure (red one represents the X-ray podophyllotoxin structure). RMSD (heavy atoms) = 0.02 to 0.85 Å.

4a

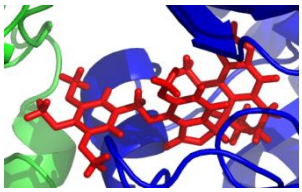

4b

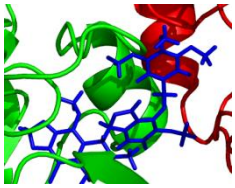

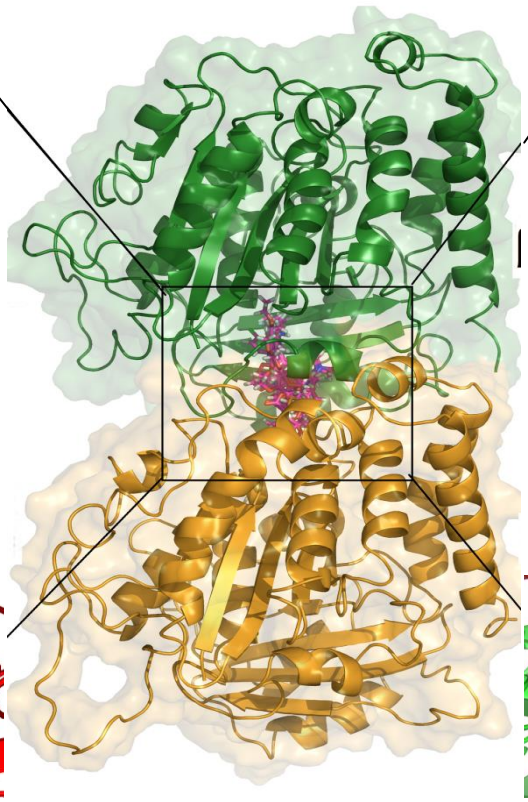

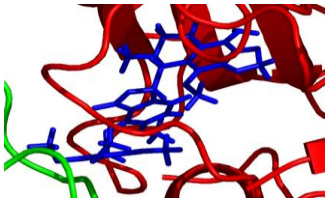

4c

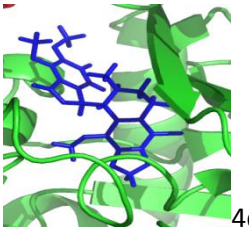

4d

4e

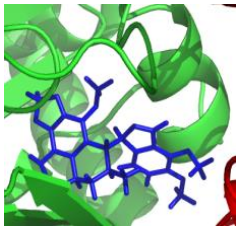

4f

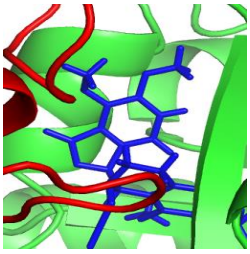

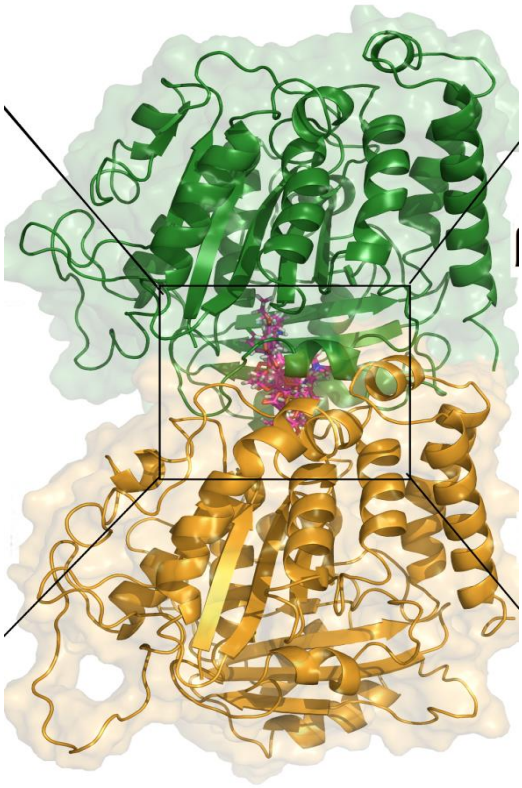

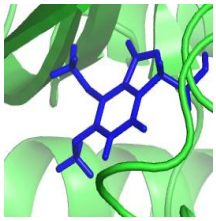

4g

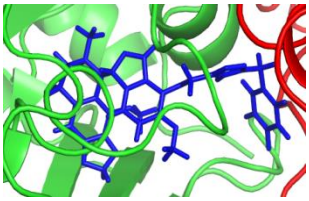

4h1

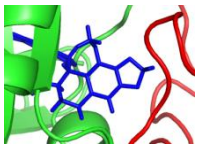

4i1

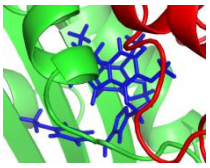

4j1

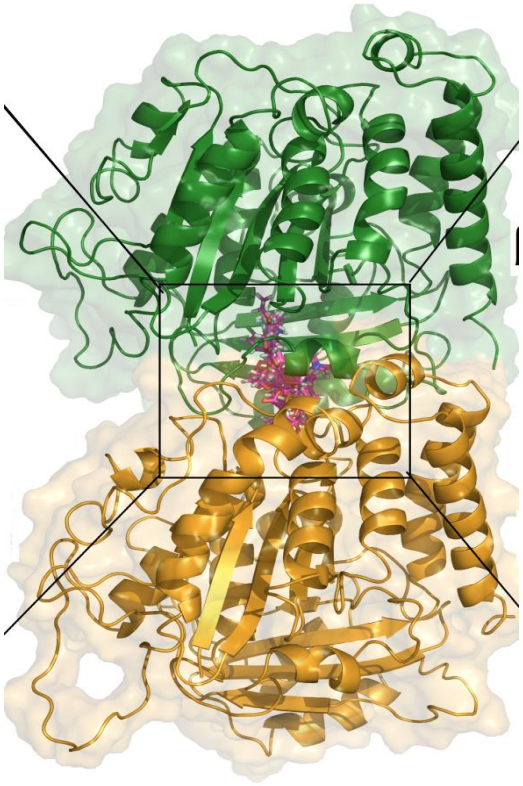

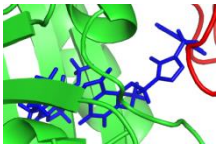

4k1

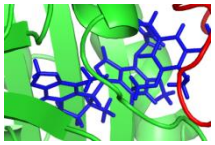

4l1

Fig 12. The newly designed noscapinoids **4a-4f** are well accommodated in the noscapinoid binding site at the interface between α- and β- tubulin. Snapshot of the ligands **4a-f** are obtained from the MM-GBSA calculation. The binding site is represented as

Macromodel surface according to residue charge (electropositive charge, blue; neutral, yellow and electronegative charge, red) as implemented in Pymol.

Fig 13. Also prepare 2D ligplot for all the 18 derivatives and put here as figure a,b,c in 3 pages. Each page consists of 6 ligplots.

For each ligand, the pose with the lowest Glide score was rescored using Prime/MM-GBSA approach. This approach is used to predict the binding free energy (ΔG_{bind}) for set of ligands to receptor. Table 4 reveals the ΔG_{bind} energy and its components of all the newly designed noscapinoids. All the derivatives showed better binding affinity, ranging from -45.12 kcal/mol to -100.75 kcal/mol. So we can conclude that the structural derivatives of noscapine used in the study is far more focused to tubulin binding site based on both Glide score and Prime/MM-GBSA approaches.

Chapter-5

Conclusion

We have compiled a library of noscapinoids (18 in total), built through structural modification of scaffold structure of natural noscapine. Docking and rescoring have been done using Prime/MM-GBSA in the work to get insights into ligand:tubulin interactions and predictive binding affinity of noscapine derivatives. In the docking simulations, the flexible docking reproduced the binding structure of crystal structures well. These experiments verified the docking protocol adopted in the work. Also the docking simulations of structurally similar inhibitors showed that the docking simulation could dock inhibitors into a receptor comparable to the crystal structure complex with podophyllotoxin. Several sets of noscapine analogues have been studied in the docking simulations. Results showed that these analogues bind in a very similar mode. The magnitude of the binding affinity can be a key factor that decides the activeness of an individual inhibitor. An energetic evaluation of the binding affinity will provide a way to estimate the activity of inhibitors. In any binding energy calculation, the correct binding structure of each ligand has to be determined first prior to binding energy estimation. Only the crystal structure of podophyllotoxin with tubulin is available. But the crystal structure of noscapine with tubulin is not available. We use flexible docking to determine the binding structure of the noscapine analogues with tubulin. Very similar binding structures were obtained for a set of analogues. The newly designed noscapinoids showed improved binding affinity compared to noscapine. Taken together these analogs indicate a great potential for further preclinical and clinical evaluation.

References

Aggarwal S, Ghosh NN, Aneja R, Joshi HC, Chandra R : A convenient synthesis of aryl-substituted N-carbamoyl/N-thiocarbamoyl narcotine and related compounds. *Helvetica Chimica Acta* 2002;85:2458-2462.

Allen, C., and Borisy, G. G. (1974). Structural polarity and directional growth of microtubules of Chlamydomonas flagella. J. Mol. Biol. 90, 381-402.

Amon, A. (1999). The spindle checkpoint. Curr. Opin. Cell Biol. 9, 69-75.

Amos, L., and Klug, A. (1974). Arrangement of subunits in flagellar microtubules. J. Cell Sci. 14, 523-549.

Aneja R, Vangapandu SN, Joshi HC: Synthesis and biological evaluation of a cyclic ether fluorinated noscapine analog. *Bioorg Med Chem* 2006;14:8352-8358.

Aneja R, Vangapandu SN, Lopus M, Chandra R, Panda D, Joshi HC : Development of a novel nitro-derivative of noscapine for the potential treatment of drug-resistant ovarian cancer and T-cell lymphoma. *Mol Pharmacol* 2006;69:1801-1809.

Aneja R, Vangapandu SN, Lopus M, Viswesarappa VG, Dhiman N, Verma A, Chandra R, Panda D, Joshi HC: Synthesis of microtubule-interfering halogenated noscapine analogs perturb mitosis in cancer cells followed by cell death. *Biochem Pharmacol* 2006;72:415-426.

Aneja, R., Kalia, V., Ahmed, R. and Joshi, H.C. (2007) Nonimmunosuppressive chemotherapy:EM011-treated mice mount normal T-cell responses to an acute lymphocytic choriomeningitis virus infection. Molecular Cancer Therapy 6, 2891-2899.

Aneja, R., Lopus, M., Zhou, J., Vangapandu, S.N., Ghaleb, A., Yao, J., Nettles, J.H., Zhou, B., Gupta, M., Panda, D., Chandra, R. and Joshi, H.C. (2006) Rational design of the microtubule-targeting anti-breast cancer drug EM015. Cancer Research 66, 3782-3791.

Aneja, R., Vangapandu, S.N., Lopus, M., Chandra, R., Panda, D. and Joshi, H.C. (2006) Development of a novel nitro-derivative of noscapine for the potential treatment of drug-resistant ovarian cancer and T-cell lymphoma. Molecular pharmacology 69, 1801-1809.

Belmont, L. D., Hyman, A. A., Sawin, K. E., and Mitchison, T. J. (1990). Real-time visualization of cell cycle-dependent changes in microtubule dynamics in cytoplasmic extracts. Cell 62, 579-589.

Bissery, M. C., Guenard, D., Gueritte-Voegelein, F., and Lavelle, F. (1991). Experimental antitumor activity of taxotere (RP 56976, NSC 628503), a taxol analogue. Cancer Res. 51, 4845-4852.

Borisy, G. G., and Taylor, E. W. (1967a). The mechanism of action of colchicine. Binding of colchicine-3H to cellular protein. J. Cell Biol. 34, 525-533.

Borisy, G. G., and Taylor, E. W. (1967b). The mechanism of action of colchicine. Colchicine binding to sea urchin eggs and the mitotic apparatus. J. Cell Biol. 34, 535-548.

Bradley, G., and Ling, V. (1994). P-glycoprotein, multidrug resistance and tumor progression. Cancer Metastasis Rev. 13, 223-233.

Brown, D. & Superti-Furga, G. (2003). Rediscovering the sweet spot in drug discovery. *Drug Discov Today.* **8:** 1067–1077.

Burkhart, C. A., Kavallaris, M., and Horwitz, S. B. (2001). The role of beta-tubulin isotypes in resistance to antimitotic drugs. Biochim. Biophys. Acta 1471, O1-O9.

Burns, R. G. (1991). Alpha-, beta-, and gamma-tubulins: sequence comparisons and structural constraints. Cell Motil. Cytoskeleton 20, 181-189.

Cahill, D. P., Lengauer, C., Yu, J., Riggins, G. J., Willson, J. K., Markowitz, S. D., Kinzler, K. W., and Vogelstein, B. (1998). Mutations of mitotic checkpoint genes in human cancers. Nature 392, 300-303.

Cavaletti, G., Tredici, G., Braga, M. and Tazzari, S. (1995) Experimental peripheral neuropathyinduced in adult rats by repeated intraperitoneal administration of taxol. Experimental neurology 133, 64-72.

Chakraborty S., Gupta S., Sarkar T., Poddar A., Pena J., Solana R., Tarazona R., Bhattacharyya B. (2004). The B-ring substituent at C-7 of colchicine and the alpha-C-terminus of tubulin communicate through the "tail-body" interaction. Proteins **57** (3): 602-609.

Chan, G. K., Jablonski, S. A., Sudakin, V., Hittle, J. C., and Yen, T. J. (1999). Human BUBR1 is a mitotic checkpoint kinase that monitors CENP-E functions at kinetochores and binds the cyclosome/APC. J. Cell Biol. 146, 941-954.

Chan, G. K., Schaar, B. T., and Yen, T. J. (1998). Characterization of the kinetochore binding domain of CENP-E reveals interactions with the kinetochore proteins CENP-F and hBUBR1. J. Cell Biol. 143, 49-63.

Chopra, R. N., Mukherjee, B. I., and Dikshit, B. B. (1930). Narcotine: its pharmacological action and therapeutic uses. Indian J. Med. Res. 18, 35-49.

Crown, J., and O'Leary, M. (2000). The taxanes: an update. Lancet 355, 1176-1178.

Dahlström, B., Mellstrand, T. and Löfdahl, C.G. (1982) Johansson M. Pharmacokinetic properties of noscapine. European journal of clinical pharmacology 22, 535-9.

Dahlstrom, B., Mellstrand, T., Lofdahl, C. G., and Johansson, M. (1982). Pharmacokinetic properties of noscapine. Eur. J. Clin. Pharmacol. 22, 535-539.

David-Pfeuty, T., Erickson, H. P., and Pantaloni, D. (1977). Guanosinetriphosphatase activity of tubulin associated with microtubule assembly. Proc. Natl. Acad. Sci. U.S.A. 74, 5372-5376.

Donehower, R.C., Rowinsky, E.K., Grochow, L.B., Longnecker, S.M. and Ettinger, D.S. (1987) Phase I trial of taxol in patients with advanced cancer. Cancer treatment reports 71, 1171-1177.

Empey, D. W., Laitinen, L. A., Young, G. A., Bye, C. E., and Hughes, D. T. (1979). Comparison of the antitussive effects of codeine phosphate 20 mg, dextromethorphan 30 mg and noscapine 30 mg using citric acid-induced cough in normal subjects. Eur. J. Clin. Pharmacol. 16, 393-397.

Fan, J., Griffiths, A. D., Lockhart, A., Cross, R. A., and Amos, L. A. (1996a). Microtubule minus ends can be labeled with a phage display antibody specific to alpha-tubulin. J. Mol. Biol. 259, 325-330.

Giannakakou, P., Gussio, R., Nogales, E., Downing, K.H., Zaharevitz, D., Bollbuck, B., Poy, G., Sackett, D., Nicolaou, K.C. and Fojo, T. (2000) A common pharmacophore for epothilone and taxanes: molecular basis for drug resistance conferred by tubulin mutations in human cancer cells. Proceedings of the National Academy of Sciences of the United States of America 97, 2904-2909

Giannakakou, P., Sackett, D. L., Kang, Y. K., Zhan, Z., Buters, J. T., Fojo, T., and Poruchynsky, M. S. (1997). Paclitaxel-resistant human ovarian cancer cells have mutant beta-tubulins that exhibit impaired paclitaxel-driven polymerization. J. Biol. Chem. 272, 17118-17125.

Giannakakou, P., Sackett, D.L., Kang, Y.K., Zhan, Z., Buters, J.T., Fojo, T. and Poruchynsky, M.S. (1997) Paclitaxel-resistant human ovarian cancer cells have mutant beta-tubulins that exhibit impaired paclitaxel-driven polymerization. The Journal of biological chemistry 272, 17118-25.

Gomeni, R., Bani, M., D'Angeli, C., Corsi, M. & Bye, A. (2001). Computer-assisted drug development (CADD): an emerging technology for designing first-time-in-man and proof-of-concept studies from preclinical experiments. *Eur J Pharm Sci.* **13:** 261–270.

Gottesman, M. M., and Pastan, I. (1993). Biochemistry of multidrug resistance mediated by the multidrug transporter. Annu. Rev. Biochem. 62, 385-427.

Guchelaar, H.J., ten Napel, C.H., de Vries, E.G. and Mulder, N.H. (1994) Clinical, toxicological and pharmaceutical aspects of the antineoplastic drug taxol. Clinical oncology (Royal College of Radiologists (Great Britain)) 6, 40-48.

Haikala, V., Sothmann, A. and Marvola, M. (1986) Comparative bioavailability and pharmacokinetics of noscapine hydrogen embonate and noscapine hydrochloride. European journal of clinical pharmacology 31, 367-369.

Hartwell, L. H., and Weinert, T. A. (1989). Checkpoints: controls that ensure the order of cell cycle events. Science 246, 629-634.

Hofer, S. and Herrmann, R. (2001) Chemotherapy for malignant brain tumors of astrocytic and oligodendroglial lineage. Journal of cancer research and clinical oncology 127, 91-105.

Hoyt, M. A., Totis, L., and Roberts, B. T. (1991). S. cerevisiae genes required for cell cycle arrest in response to loss of microtubule function. Cell 66, 507-517.

Hruban, R.H., Yardley, J.H., Donehower, R.C. and Boitnott, J.K. (1989) Taxol toxicity. Epithelial necrosis in the gastrointestinal tract associated with polymerized microtubule accumulation and mitotic arrest. Cancer 63, 1944-1950.

Idänpään-Heikkilä, J.E. (1968) Studies on the fate of 3H-noscapine in mice and rats. Annales medicinae experimentalis et biologiae Fenniae 46, 201-216.

Jin, D. Y., Spencer, F., and Jeang, K. T. (1998). Human T cell leukemia virus type 1 oncoprotein Tax targets the human mitotic checkpoint protein MAD1. Cell 93, 81-91.

Jordan, M. A., and Wilson, L. (1999). The use and action of drugs in analyzing mitosis. Methods Cell Biol. 61, 267-295.

Joshi, H. C. (1998). Microtubule dynamics in living cells. Curr. Opin. Cell Biol. 10, 35-44.

Joshi, H.C. and Cleveland, D.W. (1990) Diversity among tubulin subunits: toward what functional end? Cell motility and the cytoskeleton 16, 159-63.

Karlsson, M. O., Dahlstrom, B., Eckernas, S. A., Johansson, M., and Alm, A. T. (1990). Pharmacokinetics of oral noscapine. Eur. J. Clin. Pharmacol. 39, 275-279.

Karlsson, M. O., Dahlstrom, B., Eckernas, S. A., Johansson, M., and Alm, A. T. (1990). Pharmacokinetics of oral noscapine. Eur. J. Clin. Pharmacol. 39, 275-279.

Karlsson, M.O., Dahlström, B., Eckernäs, S.A., Johansson, M and Alm, A.T. (1990) Pharmacokinetics of oral noscapine. European journal of clinical pharmacology 39, 275-9.

Ke, Y., Ye, K., Grossniklaus, H.E., Archer, D.R., Joshi, H.C. and Kapp, J.A. (2000) Noscapine inhibits tumor growth with little toxicity to normal tissues or inhibition of immune responses. Cancer immunology and immunotherapy 49, 217-225.

Krishna, R. and Mayer, L.D. (2000) Multidrug resistance (MDR) in cancer. Mechanisms, reversal using modulators of MDR and the role of MDR modulators in influencing the pharmacokinetics of anticancer drugs. European journal of pharmaceutical sciences 11, 265-283.

Landen, J.W., Hau, V., Wang, M., Davis, T., Ciliax, B., Wainer, B.H., Van Meir, E.G., Glass, J.D., Joshi, H.C. and Archer, D.R. (2004) Noscapine crosses the blood-brain barrier and inhibits glioblastoma growth. Clinical cancer research 10, 5187-5201.

Landen, J.W., Lang, R., McMahon, S.J., Rusan, N.M., Yvon, A.M., Adams, A.W., Sorcinelli, M.D., Campbell, R., Bonaccorsi, P., Ansel, J.C., Archer, D.R., Wadsworth, P., Armstrong, C.A. and Joshi, H.C. (2002) Noscapine alters microtubule dynamics in living cells and inhibits the progression of melanoma. Cancer research 62, 4109-4114.

Lasagna, L., Owens, A.H. Jr., Shnider, B.I. and Gold, G.L. (1961) Toxicity after large doses of noscapine. Cancer chemotherapy reports. Part 1 15, 33-34.

Li, R., and Murray, A. W. (1991). Feedback control of mitosis in budding yeast. Cell 66, 519-531.

Li, Y., and Benezra, R. (1996). Identification of a human mitotic checkpoint gene:hsMAD2. Science 274, 246–248.

Lipton, R.B., Apfel, S.C., Dutcher, J.P., Rosenberg, R., Kaplan, J., Berger, A., Einzig, A.I., Wiernik, P. and Schaumburg, H.H. (1989) Taxol produces a predominantly sensory neuropathy. Neurology 39, 368-373.

Lodish, H.; Baltimore, D.; Berk, A.; Zipursky, S.L.; Matsudaira, P.; Darnell, J (1999). *Molecular Cell Biology*. W.H. Freeman, New York.

Ludueña, R.F. (1998) Multiple forms of tubulin: different gene products and covalent modifications. International review of cytology 178, 207-275.

MacNeal, R. K., and Purich, D. L. (1978). Stoichiometry and role of GTP hydrolysis in bovine neurotubule assembly. J. Biol. Chem. 253, 4683-4687.

Manchester, K. L. (1995). Boveri, Theodor and the origin of malignant-tumors. Trends Cell Biol. 5, 384-387.

Mandelkow, E. M., Schultheiss, R., Rapp, R., Muller, M., and Mandelkow, E. (1986). On the surface lattice of microtubules: helix starts, protofilament number, seam, and handedness. J. Cell Biol. 102, 1067-1073.

Margolis, R. L., and Wilson, L. (1978). Opposite end assembly and disassembly of microtubules at steady state in vitro. Cell 13, 1-8.

Martindale, P. (1977) In: Wade (ed) the extra pharmacopoeia. Pharmaceutical Press, London, p1250

Martinez-Exposito, M. J., Kaplan, K. B., Copeland, J., and Sorger, P. K. (1999). Retention of the BUB3 checkpoint protein on lagging chromosomes. Proc. Natl. Acad. Sci. U.S.A. 96, 8493-8498.

Mazia, D. (1961). Mitosis. In "The Cell" (J. Brachet and A. E. Mirsky, eds.), Vol. 3, pp. 77-142. Academic Press, New York.

McIntosh, J. R. (1991). Structural and mechanical control of mitotic progression. Cold Spring Harbor Symp. Quant. Biol. 56, 613-619.

Michel, L. S., Liberal, V., Chatterjee, A., Kirchwegger, R., Pasche, B., Gerald, W., Dobles, M., Sorger, P. K., Murty, V. V., and Benezra, R. (2001). MAD2 haplo-insufficiency causes premature anaphase and chromosome instability in mammalian cells. Nature 409, 355-359.

Mitchison, T., and Kirschner, M. (1984a). Microtubule assembly nucleated by isolated centrosomes. Nature 312, 232-237.

Mitchison, T., and Kirschner, M. (1984b). Dynamic instability of microtubule growth. Nature 312, 237-242.

Nicklas, R. B. (1997). How cells get the right chromosomes. Science 275, 632-637.

Nicolaou, K.C., Yang, Z., Liu, J.J., Ueno, H., Nantermet, P.G., Guy, R.K., Claiborne, C.F., Renaud, J., Couladouros, E.A. and Paulvannan, K., et al. (1994) Total synthesis of taxol. Nature 367, 630-634.

Nogales E., Wolf SG., Downing KH. (1998). Structure of the alpha beta tubulin dimer by electron crystallography. Nature **391** (6663):199-203.

Perkin, W., H. and Robinson, R. (1910) Synthesis of dl-narcotine (gnoccopine). Priliminary note. Proceedings of Chemical Society 26, 48

Rai SS., Wolff J. (1998). The C terminus of beta-tubulin regulates vinblastine-induced tubulin polymerization. Proceedings of the National Academy of Sciences USA **95** (8): 4253-4257.

Rieder, C. L., and Salmon, E. D. (1994). Motile kinetochores and polar ejection forces dictate chromosome position on the vertebrate mitotic spindle. J. Cell Biol. 124, 223-233.

Rieder, C. L., and Salmon, E. D. (1998). The vertebrate cell kinetochore and its roles during mitosis. Trends Cell Biol. 8, 310-318.

Rowinsky, E. K. (1997). The development and clinical utility of the taxane class of antimicrotubule chemotherapy agents. Annu. Rev. Med. 48, 353-374.

Rowinsky, E.K., Cazenave, L.A. and Donehower, R.C. (1990) Taxol: a novel investigational antimicrotubule agent. Journal of the National Cancer Institute 82, 1247-1259.

Rudner, A. D., and Murray, A. W. (1996). The spindle assembly checkpoint. Curr. Opin. Cell Biol. 8, 773-780.

Saxton, W. M., Stemple, D. L., Leslie, R. J., Salmon, E. D., Zavortink, M., and McIntosh, J. R. (1984). Tubulin dynamics in cultured mammalian cells. J. Cell Biol. 99, 2175-2186.

Schiff, P. B., and Horwitz, S. B. (1980). Taxol stabilizes microtubules in mouse fibroblast cells. Proc. Natl. Acad. Sci. U.S.A. 77, 1561-1565.

Schulze, E., and Kirschner, M. (1986). Microtubule dynamics in interphase cells. J. Cell Biol. 102, 1020-1031.

Sluder, G., and McCollum, D. (2000). The mad ways of meiosis. Science 289, 254-255.

Song, Y. H., and Mandelkow, E. (1995). The anatomy of flagellar microtubules: polarity, seam, junctions, and lattice. J. Cell Biol. 128, 81-94.

Spiegelman, B. M., Penningroth, S. M., and Kirschner, M. W. (1977). Turnover of tubulin and the N site GTP in Chinese hamster ovary cells. Cell 12, 587-600.

Stewart, Z.A., Mays, D. and Pietenpol, J.A. (1999) Defective G1-S cell cycle checkpoint function sensitizes cells to microtubule inhibitor-induced apoptosis. Cancer research 59, 3831-3837.

Takahashi, T., Haruki, N., Nomoto, S., Masuda, A., Saji, S., and Osada, H. (1999). Identification of frequent impairment of the mitotic checkpoint and molecular analysis of the mitotic checkpoint genes, hsMAD2 and p55CDC, in human lung cancers. Oncogene 18, 4295-4300.

Taylor, S. S., and McKeon, F. (1997). Kinetochore localization of murine Bub1 is required for normal mitotic timing and checkpoint response to spindle damage. Cell 89, 727-735.

Taylor, S. S., Ha, E., and McKeon, F. (1998). The human homologue of Bub3 is required for kinetochore localization and a Mad3/Bub1-related protein kinase. J. Cell Biol. 142, 1–11.

Tiveron, C., Hartley-Asp, B., Johansson, C.J. and Pacchierotti, F. (1993) Noscapine does not show aneugenic activity in mouse oocytes. Mutagenesis 8, 311-315.

van Tellingen, O., Sips, J. H., Beijnen, J. H., Bult, A., and Nooijen, W. J. (1992). Pharmacology, bio-analysis and pharmacokinetics of the vinca alkaloids and semi-synthetic derivatives (review). Anticancer Res. 12, 1699-1715.

Veselovsky, A. V. & Ivanov, A. S. (2003). Strategy of computer-aided drug design. *Curr Drug Targets Infect Disord.* **3:** 33–40.

Walker, R. A., O'Brien, E. T., Pryer, N. K., Soboeiro, M. F., Voter, W. A., Erickson, H. P., and Salmon, E. D. (1988). Dynamic instability of individual microtubules analyzed by video light microscopy: rate constants and transition frequencies. J. Cell Biol. 107, 1437-1448.

Wang, X., Jin, D. Y., Ng, R. W., Feng, H., Wong, Y. C., Cheung, A. L., and Tsao, S. W. (2002). Significance of MAD2 Expression to Mitotic Checkpoint Control in Ovarian Cancer Cells. Cancer Res. 62, 1662-1668.

Warolin, C., and Pierre-Jean Robiquet (1999) Revue d'histoire de la pharmacie 47, 97-110

Waters, J. C., Chen, R. H., Murray, A. W., and Salmon, E. D. (1998). Localization of Mad2 to kinetochores depends on microtubule attachment, not tension. J. Cell Biol. 141, 1181-1191.

Weisenberg, R. C., Borisy, G. G., and Taylor, E. W. (1968). The colchicine-binding protein of mammalian brain and its relation to microtubules. Biochemistry 7, 4466-4479.

Weisenberg, R. C., Borisy, G. G., and Taylor, E. W. (1968). The colchicine-binding protein of mammalian brain and its relation to microtubules. Biochemistry 7, 4466-4479.

Weiss, E., and Winey, M. (1996). The S. cerevisiae SPB duplication gene MPS1 is part of a mitotic checkpoint. J. Cell Biol. 132, 111-123.

Wells, W. A. E. (1996). The spindle-assembly checkpoint: Aiming for a perfect mitosis, every time. Trends Cell Biol. 6, 228-234.

Wiernik, P.H., Schwartz, E.L., Strauman, J.J., Dutcher, J.P., Lipton, R.B. and Paietta, E. (1987) Phase I clinical and pharmacokinetic study of taxol. Cancer Research 47, 2486-2493.

Winter, C. A., and Flataker, L. (1954). Antitussive compounds testing methods and results. J. Pharmacol. Exp. Ther. 112, 99-108.

Workman, P. (2003). How much gets there and what does it do?: The need for better pharmacokinetic and pharmacodynamic endpoints in contemporary drug discovery and development. *Curr Pharm Des.* **9:** 891–902.

Ye, K., Ke, Y., Keshava, N., Shanks, J., Kapp, J. A., Tekmal, R. R., Petros, J., and Joshi, H. C. (1998). Opium alkaloid noscapine is an antitumor agent that arrests metaphase and induces apoptosis in dividing cells. Proc. Natl. Acad. Sci. U.S.A. 95, 1601-1606.

Zhou, J., Gupta, K., Aggarwal, S., Aneja, R., Chandra, R., Panda, D. and Joshi, H.C. (2003) Brominated derivatives of noscapine are potent microtubule-interfering agents that perturb mitosis and inhibit cell proliferation. Molecular pharmacology 63, 799-807.

Zhou, J., Gupta, K., Aggarwal, S., Aneja, R., Chandra, R., Panda, D. and Joshi, H.C. (2003) Brominated derivatives of noscapine are potent microtubule-interfering agents that perturb mitosis and inhibit cell proliferation. Molecular pharmacology 63, 799-807.

Zhou, J., Gupta, K., Yao, J., Ye, K., Panda, D., Giannakakou, P. and Joshi, H.C. (2002) Paclitaxel-resistant human ovarian cancer cells undergo c-Jun NH2-terminal kinase-mediated apoptosis in response to noscapine. The Journal of biological chemistry 277, 39777-39785.

Zhou, J., Liu, M., Aneja, R., Chandra, R., Lage, H. and Joshi, H.C. (2006) Reversal of P-glycoprotein-mediated multidrug resistance in cancer cells by the c-Jun NH2-terminal kinase. Cancer Research 66, 445-452.